Theoretical Studies of Oxidative Addition and Reductive Elimination. 3. C-H and C-C Reductive Coupling from Palladium and Platinum Bis(phosphine) Complexes

John J. Low† and William A. Goddard, III*

Contribution No. 7180 from the Arthur Amos Noyes Laboratory of Chemical Physics, California Institute of Technology, Pasadena, California 91125. *Received May 1, 1985*

Abstract: Ab initio calculations were carried out on $Pt(CH_3)_2(Cl)_2(PH_3)_2$ and on various $Mt(R_1)(R_2)(PH_3)_2$ complexes (where Mt = Pd or Pt; R_1, R_2 = H or CH_3) in order to elucidate the differences in reductive H–C and C–C coupling from Pd(II), Pt(II), and Pt(IV) complexes. These studies explain why (1) reductive C–C coupling is facile for Pd(II), favorable for Pt(IV), and unobserved for Pt(II) systems, while (2) reductive H–C coupling is facile for Pt(II) and Pd(II) systems, and (3) oxidative addition is favorable only for the addition of H_2 to Pt(0) systems.

I. Introduction

In spite of the importance of oxidative addition and reductive elimination in organometallic chemistry,[1] a fundamental understanding of the electronic structure of these reactions is only just emerging.[2-5] Some of the experimental observations are as follows, focusing only on Pd and Pt complexes:

(i) C–C coupling from Pd dialkylbis(phosphines)[6]

$$Pd(CH_3)_2(PR_3)_2 \rightarrow Pd(PR_3)_2 + CH_3{-}CH_3 \qquad (1)$$

and from dimethyl, trimethyl, and tetramethyl Pt(IV)[7] complexes, e.g.,

$$Pt(CH_3)_2(Cl)_2(PR_3)_2 \rightarrow Pt(Cl)_2(PR_3)_2 + CH_3{-}CH_3 \qquad (2)$$

is intramolecular and consistent with a concerted process. Conversely, (ii) Pt dialkyls tend to decompose through β-hydride elimination[8] if this pathway is available, even though direct C–C reductive coupling is thermodynamically favored (by 11 kcal/mol):[9]

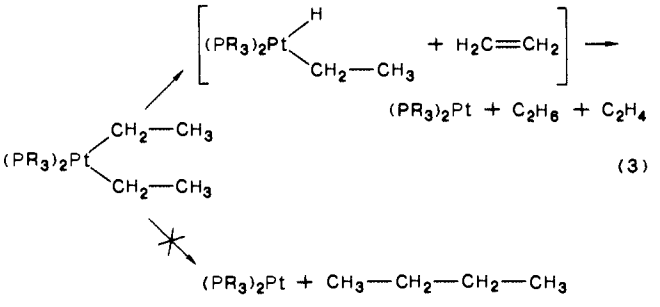

(3)

(iii) $Pt(CH_3)_2(PR_3)_2$ complexes are thus very stable and have never been observed to undergo reductive elimination,[10] while (iv) Pt(II) biphenyls, on the other hand, reductively couple to form C–C bonds.[11] (v) In contrast, reductive H–C coupling occurs readily from Pt(II) complexes,[12,13]

$$Pt(H)(CH_3)(PR_3)_2 \rightarrow Pt(PR_3)_2 + CH_4 \qquad (4)$$

and presumably would also occur from analogous Pd(II) and Pt(IV) complexes should they be formed. (vi) On the other hand, the reverse (oxidative addition) reaction to (1), (2), and (4) has not been observed, and oxidative addition has been observed[14] only for

$$Pt(PR_3)_2 + H_2 \rightarrow Pt(H)_2(PR_3)_2 \qquad (5)$$

(and not for the analogous Pd(II) species).

In order to elucidate the general trends about reductive elimination/oxidative addition, we have carried out ab initio calculations for the species $Pt(CH_3)_2(PH_3)_2$ (**1**), $Pd(CH_3)_2(PH_3)_2$ (**2**), $Pt(Cl)_2(CH_3)_2(PH_3)_2$ (**3**), $Pt(Cl)_2(PH_3)_2$ (**4**), $Pt(H)(CH_3)(PH_3)_2$ (**5**), and $Pt(H)_2(PH_3)_2$ (**6**) and for the reductive coupling products $Pt(PH_3)_2$ (**7**) and $Pd(PH_3)_2$ (**8**). These data plus the results from previous studies[2] on the transition states and barriers for reductive

Table 1. Mulliken Populations for the GVB Bond Pairs of $M(R_1)(R_2)$[a]

	populations in GVB bond orbitals	
	M–CH_3	M–H or M–Cl
1, $Pt(CH_3)_2(PH_3)_2$	$s^{0.23}p^{0.10}d^{0.49}C^{0.17}$	
	$(sp)^{-0.03}d^{0.13}Cs^{0.18}p^{0.71}$	
2, $Pd(CH_3)_2(PH_3)_2$	$s^{0.17}p^{0.07}d^{0.49}C^{0.24}$	
	$(sp)^{-0.02}d^{0.15}Cs^{0.18}p^{0.58}$	
3, $Pt(CH_3)_2(Cl)_2(PH_3)_2$	$s^{0.17}p^{0.07}d^{0.69}C^{0.04}$	$s^{0.19}p^{0.25}d^{0.21}Cl^{0.37}$
	$(sp)^{0.00}d^{0.19}Cs^{0.11}p^{0.67}$	$(sp)^{-0.06}d^{0.07}Cls^{0.03}p^{0.93}$
4, $Pt(Cl)_2(PH_3)_2$		$s^{0.21}p^{0.11}d^{0.37}Cl^{0.27}$
		$(sp)^{-0.03}d^{0.06}Cls^{0.01}p^{0.95}$
5, $Pt(H)(CH_3)(PH_3)_2$	$s^{0.24}p^{0.11}d^{0.49}C^{0.15}$	$s^{0.27}p^{0.13}d^{0.51}H^{0.09}$
	$(sp)^{-0.04}d^{0.13}Cs^{0.18}p^{0.72}$	$(sp)^{-0.02}d^{0.16}C^{0.01}H^{0.85}$
$Pt(H)_2$[b]		$s^{0.29}p^{0.02}d^{0.63}H^{0.07}$
		$(sp)^{0.02}d^{0.19}H^{0.80}$
$Pt(H)(CH_3)$[b]	$s^{0.26}p^{0.01}d^{0.64}C^{0.09}$	$s^{0.30}p^{0.02}d^{0.60}H^{0.08}$
	$(sp)^{0.01}d^{0.16}Cs^{0.12}p^{0.70}$	$(sp)^{0.01}d^{0.18}H^{0.80}$
$Pt(CH_3)_2$[b]	$s^{0.27}p^{0.01}d^{0.62}C^{0.10}$	
	$(sp)^{0.00}d^{0.15}Cs^{0.14}p^{0.70}$	
$Pd(CH_3)_2$[b]	$s^{0.16}p^{0.03}d^{0.55}C^{0.24}$	
	$(sp)^{0.01}d^{0.20}Cs^{0.28}p^{0.52}$	

[a] For each bond there are two listings: the top one is the metal-like GVB orbital and the bottom one is the ligand-like orbital. [b] Reference 2c.

† Current address: Allied-Signal Engineered Materials Research Center, 50 East Algonquin Road, Des Plaines, Illinois 60017.

(1) Collman, J. P.; Hegedus, L. S. *Principles and Applications of Organotransition Metal Chemistry*; University Science Books: Mill Valley, CA, 1980; Chapter 4.

(2) (a) Low, J. J.; Goddard, W. A., III *J. Am. Chem. Soc.* **1984**, *106*, 6928-6937. (b) Low, J. J.; Goddard, W. A., III *J. Am. Chem. Soc.* **1984**, *106*, 8321-8322. (c) Low, J. J.; Goddard, W. A., III *Organometallics* **1986**, *5*, 609-622.

(3) (a) Tatsumi, K.; Hoffmann, R.; Yamamoto, A.; Stille, J. K. *Bull. Chem. Soc. Jpn.* **1981**, *54*, 1857-1867. (b) Komiya, S.; Albright, T. A.; Hoffmann, R.; Kochi, J. K. *J. Am. Chem. Soc.* **1976**, *98*, 7255-7265. (c) Saillard, J.; Hoffmann, R. *J. Am. Chem. Soc.* **1984**, *106*, 2006-2026. (d) Tatsumi, K.; Nakamura, A.; Komiya, S.; Yamamoto, A.; Yamamoto, T. *J. Am. Chem. Soc.* **1984**, *106*, 8181-8188.

(4) (a) Kitaura, K.; Obara, S.; Morokuma, K. *J. Am. Chem. Soc.* **1981**, *103*, 2891-2893. (b) Noell, J. O.; Hay, P. J. *Inorg. Chem.* **1982**, *21*, 14-19. (c) Noell, J. O.; Hay, P. J. *J. Am. Chem. Soc.* **1982**, *104*, 4578-4584. (d) Hay, P. J. *Chem. Phys. Lett.* **1984**, *103*, 466-469. (e) Åkermark, B.; Johansen, H.; Roos, B.; Wahlgren, U. *J. Am. Chem. Soc.* **1979**, *101*, 5876-5883. (f) Sevin, A. *Nouv. J. Chim.* **1981**, *5*, 233-241. (g) Dedieu, A.; Strich, A. *Inorg. Chem.* **1979**, *18*, 2940-2943. (h) Balazs, A. C.; Johnson, K. H.; Whitesides, G. M. *Inorg. Chem.* **1982**, *21*, 2162-2174. (i) Gritsenko, O. V.; Bagatur'yants, A. A.; Moiseev, I. I.; Kazanskii, V. B.; Kalechits, I. V. *Kinet. Katal.* **1981**, *22*, 354-358. (j) Gritsenko, O. V.; Bagatur'yants, A. A.; Moiseev, I. I.; Kalechits, I. V. *Kinet. Katal.* **1981**, *22*, 1431-1437. (k) Obara, S.; Kitaura, K.; Morokuma, K. *J. Am. Chem. Soc.* **1984**, *106*, 7482-7492.

(5) (a) Blomberg, M. R. A.; Siegbahn, P. E. M. *J. Chem. Phys.* **1983**, *78*, 986-987. (b) Blomberg, M. R. A.; Brandemark, U.; Pettersson, L.; Siegbahn, P. E. M. *Int. J. Quantum. Chem.* **1983**, *28*, 855-863. (c) Blomberg, M. R. A.; Brandemark, U.; Siegbahn, P. E. M. *J. Am. Chem. Soc.* **1983**, *105*, 5557-5563. (d) Siegbahn, P. E. M.; Blomberg, M. R. A.; Bauschlicher, C. W., Jr. *J. Chem. Phys.* **1984**, *81*, 1373-1382. (e) Brandemark, U. B.; Blomberg, M. R. A.; Petersson, L. G. M.; Siegbahn, P. E. M. *J. Phys. Chem.* **1984**, *88*, 4617-4621.

0002-7863/86/1508-6115$01.50/0

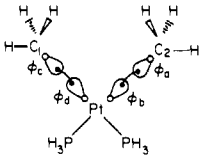

Right Pt-C Bond Pair

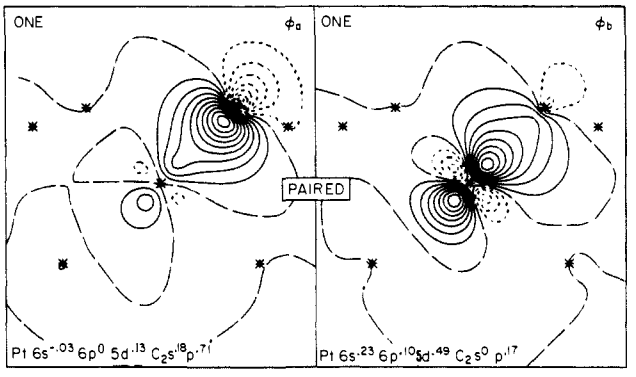

Left Pt-C Bond Poir

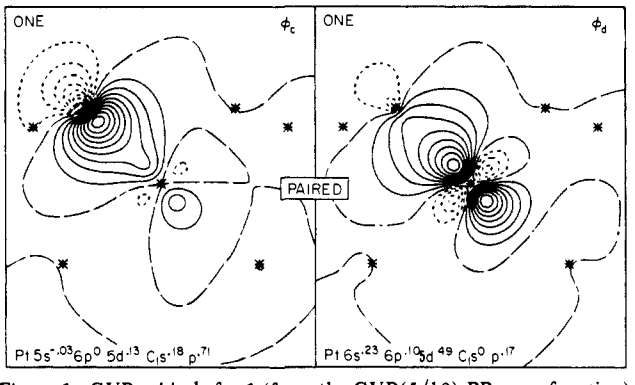

Figure 1. GVB orbitals for **1** (from the GVB(5/10)-PP wave function). Nuclei in the plane are indicated by asterisks. Positive contours are solid, negative contours are dotted, and nodal lines are long dashes. The spacing between contours is 0.05 au. Analysis of each GVB orbital in terms of a Mulliken population is shown.

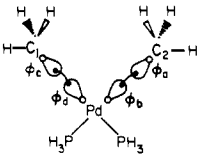

Right Pd-C Bond

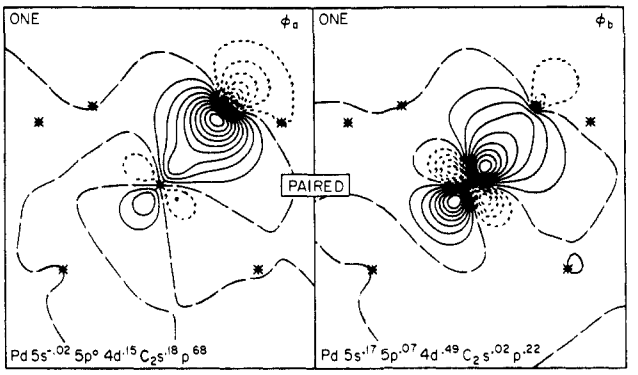

Left Pd-C Bond

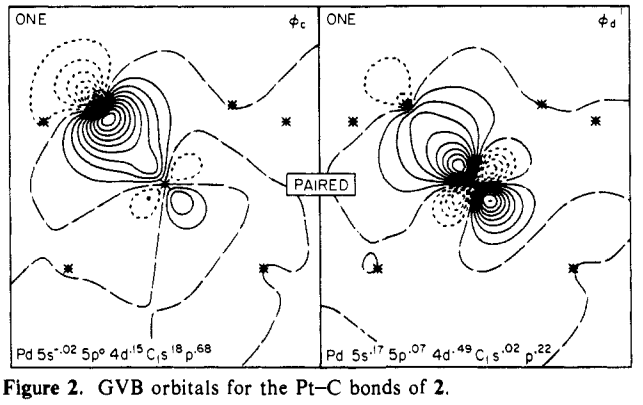

Figure 2. GVB orbitals for the Pt–C bonds of **2**.

coupling from $Mt(H)_2$, $Mt(H)(CH_3)$, and $Mt(CH_3)_2$ complexes (where Mt = Pd or Pt) are used to estimate the energetics and barriers for various reductive coupling processes in palladium and platinum bis(phosphine) complexes.

Table II. Mulliken Populations for Platinum and Palladium Bis(phosphine) Complexes

	populations					
complex	M sp	M d	CH_3	H	PH_3	Cl
1, $Pt(CH_3)_2(PH_3)_2$	0.73	8.89	9.13		8.06	
2, $Pd(CH_3)_2(PH_3)_2$	0.33	9.09	9.20		8.10	
3, $Pt(CH_3)_2(Cl)_2(PH_3)_2$	1.12	8.57	8.86		8.02	7.28
4, $Pt(Cl)_2(PH_3)_2$	0.80	8.83			7.92	7.25
5, $Pt(H)(CH_3)(PH_3)_2$	0.85	8.99	9.12	0.93	8.05[a]	
6, $Pt(H)_2(PH_3)_2$	0.96	9.10		0.98		
7, $Pt(PH_3)_2$	0.38	9.51			8.07	
8, $Pd(PH_3)_2$	0.19	9.63			8.09	
$Pt(H)_2$[b]	1.16	9.15		0.85		
$Pt(H)(CH_3)$[b]	1.05	9.03	9.04	0.89		
$Pt(CH_3)_2$[b]	0.97	8.91	9.06			
$Pd(CH_3)_2$[b]	0.60	9.15	9.13			

[a] This is the average occupation of the PH_3 groups in this complex. The PH_3 group trans to CH_3 has 8.04 e$^-$ and the PH_3 group trans to H has 8.06 e$^-$. [b] Reference c.

II. Summary of Results

A. Nature of the Chemical Bonds. As a basis for understanding the differences in energetics for C–C, C–H, and H–H reductive coupling from Pt(II), Pd(II), and Pt(IV) complexes, we first develop a qualitative picture for the bonding in these systems.

(6) (a) Gillie, A.; Stille, J. K. *J. Am. Chem. Soc.* **1980**, *102*, 4933–4941. (b) Loar, M. K.; Stille, J. K. *J. Am. Chem. Soc.* **1981**, *103*, 4174–4181. (c) Moravskiy, A.; Stille, J. K. *J. Am. Chem. Soc.* **1981**, *103*, 4182–4186. (d) Ozawa, F.; Ito, T.; Nakamura, Y.; Yamamoto, A. *Bull. Chem. Soc. Jpn.* **1981**, *54*, 1868–1880.

(7) (a) Ruddick, J. D.; Shaw, B. L. *J. Chem. Soc. A* **1969**, 2969–2970. (b) Brown, M. P.; Puddephat, R. J.; Upton, C. E. E. *J. Chem. Soc., Dalton Trans.* **1974**, 2457–2465. (c) Appleton, T. G.; Clark, H. C.; Manzer, L. E. *J. Organomet. Chem.* **1974**, *65*, 275–287.

(8) (a) Whitesides, G. M.; Gaasch, J. F.; Stedronsky, E. R. *J. Am. Chem. Soc.* **1972**, *94*, 5258–5270. (b) McDermott, J. X.; White, J. F.; Whitesides, G. M. *J. Am. Chem. Soc.* **1984**, *98*, 6521–6528. (c) Young, G. B.; Whitesides, G. M. *J. Am. Chem. Soc.* **1978**, *100*, 5808–5815. (d) McCarthy, T. J.; Nuzzo, R. G.; Whitesides, G. M. *J. Am. Chem. Soc.* **1981**, *103*, 1676–1678. (e) McCarthy, T. J.; Nuzzo, R. G.; Whitesides, G. M. *J. Am. Chem.* **1981**, *103*, 3396–3403. (f) Nuzzo, R. G.; McCarthy, T. J.; Whitesides, G. M. *J. Am. Chem. Soc.* **1981**, *103*, 3404–3410. (g) Komiya, S.; Morimoto, Y.; Yamamoto, A.; Yamamoto, T. *Organometallics* **1981**, *1*, 1528–1536.

(9) (a) $PtEt_2(PEt_3)_2$ is known to β-hydride eliminate to give ethylene ($\Delta H_f^0{}_{300}$ = 12.5 kcal/mol, S_{300} = 52.4 eu) and ethane ($\Delta H_f^0{}_{300}$ = −20.2 kcal/mol, S_{300} = 54.9 eu) rather than to reductively eliminate to give *n*-butane ($\Delta H_f^0{}_{300}$ = −30.2 kcal/mol, S_{300} = 74.1 eu) even though *n*-propane is the thermodynamically favored product (ΔH_{300} = −22.5, ΔS_{300} = −33.2 eu, ΔG_{300} = −12.5 kcal/mol for $C_2H_4 + C_2H_6 \rightarrow n\text{-}C_4H_{10}$). The $\Delta H_f^0{}_{300}$ and $S^0{}_{300}$ were taken from ref 9b. (b) Benson, S. W. *Thermochemical Kinetics*, 2nd ed.; Wiley: New York, 1976; p 295.

(10) Chatt, J.; Shaw, B. L. *J. Chem. Soc.* **1959**, 705–716.

(11) (a) Braterman, P. S.; Cross, R. J.; Young, G. B. *J. Chem. Soc., Dalton Trans.* **1976**, 1306–1309. (b) Braterman, P. S.; Cross, R. J.; Young, G. B. *J. Chem. Soc., Dalton Trans.* **1976**, 1310–1314. (c) Braterman, P. S.; Cross, R. J.; Young, G. B. *J. Chem. Soc., Dalton Trans.* **1977**, 1892–1897.

(12) (a) Abis, L.; Sen, A.; Halpern, J. *J. Am. Chem. Soc.* **1978**, *100*, 2915–2916. (b) Halpern, J. *Acc. Chem. Res.* **1982**, *15*, 332–338.

(13) Michelin, R. A.; Faglia, S.; Uguagliati, P. *Inorg. Chem.* **1983**, *22*, 1831–1834.

(14) Paonessa, R. S.; Trogler, W. C. *J. Am. Chem. Soc.* **1982**, *104*, 1138–1140.

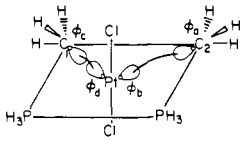

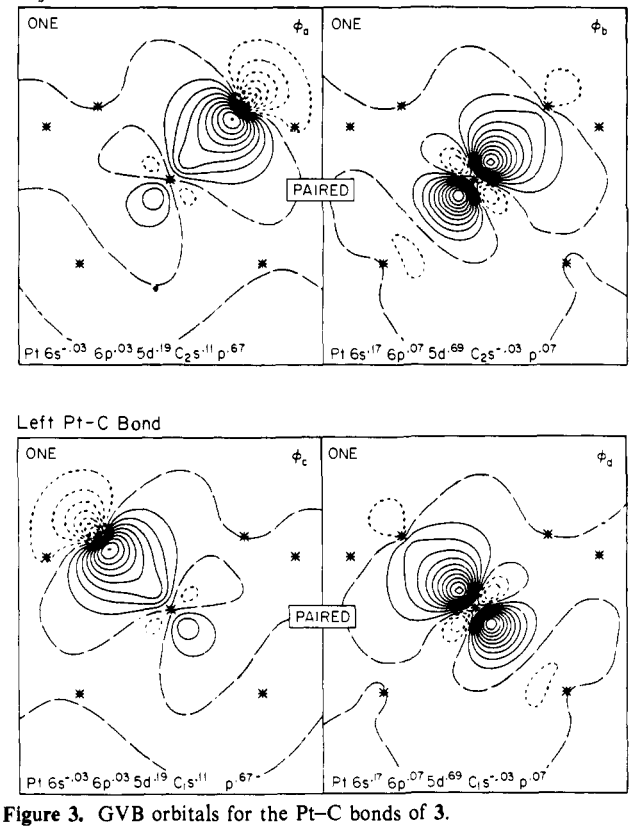

Figure 3. GVB orbitals for the Pt–C bonds of **3**.

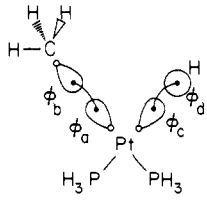

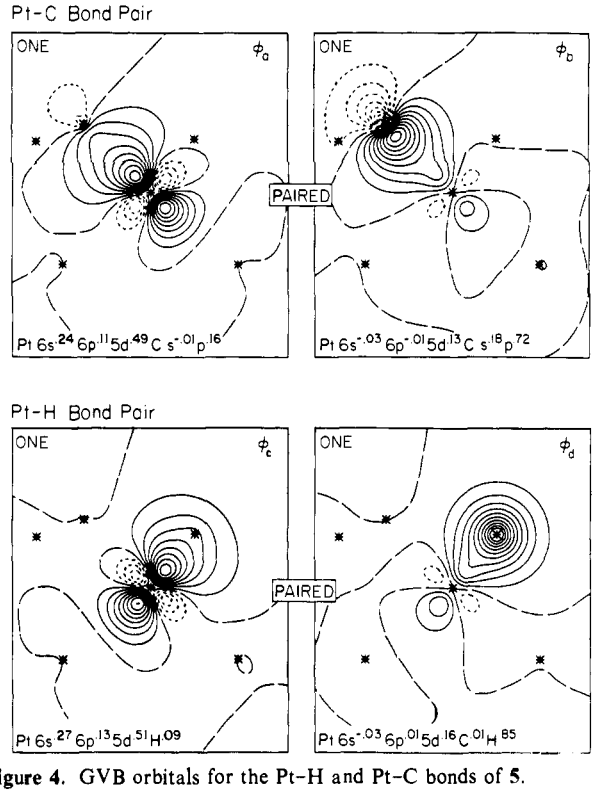

Figure 4. GVB orbitals for the Pt–H and Pt–C bonds of **5**.

1. Mt(II) Systems. The Mt–CH_3 bond orbitals (from GVB calculations) of **1–3** and **5** are shown in Figures 1–4, the Pt–Cl orbitals of **3** and **4** are shown in Figures 5 and 6, and the Pt–H orbital of **5** is shown in Figure 4. The GVB orbitals are analyzed in terms of Mulliken populations in Table I and in Figures 1–6; total populations are given in Table II. The overall qualitative description is as follows:

(1) The Mt–CH_3 bonds are covalent, with one electron in an sp^3 hybrid orbital on the CH_3 and one electron in an spd hybrid orbital (60–75% d) mainly on the metal.

(2) The Mt–H bonds are covalent, with one electron in an H 1s orbital and one electron in an spd hybrid orbital on the metal.

(3) The Mt–Cl bonds are partially ionic, with one electron in a Cl p_z orbital and the other electron in an orbital that is partly on the Cl and partly on the metal (spd hybrid with 30–50% d character).

(4) There are generally about 10 electrons on the metal with character corresponding to either (i) the atomic d^{10} configuration for **7** and **8** (generally denoted as Mt(0)), (ii) the atomic s^1d^9 configuration for **1**, **2**, and **4–6** (generally denoted as Mt(II)), or (iii) the atomic s^2d^8 configuration for **3** (generally denoted as Mt(IV)).

This focus on the 10-electron atomic configuration on the metal arises naturally from the generalized valence bond description, and we find that it provides a means for quantitative comparison of the various reaction energetics.

A more quantitative analysis of the character in the GVB orbitals is as follows (see Tables I and II). For the Pt–CH_3 bond of **1**, the metal orbital is 82% on the Pt and 17% on the C. The metal part of this orbital is 60% d, 28% s, and 12% p character, very similar to other Mt–C and Mt–H bonds.[15] The methyl orbital of the Pt–CH_3 bond pair is 89% on the C atom (18% s and 71% p or s^1p^4). The HCH bond angles (108°, 108°, and 110°) are very close to the tetrahedral bond angles expected for the sp^3 carbon. These orbitals are similar to the bond orbitals of $Pt(CH_3)_2$, where the metal orbital has 90% Pt character (69% d, 30% s, and 1% p). The carbon in the methyl group in this complex is also sp^3-like (18% s and 71% p or s^1p^4), with H–C–H bond angles of 109°, 109°, and 110°.[2c] The preference for ~60% d character in covalent metal–carbon and metal–hydrogen bonds was also observed in $Ti(H)_2(Cl)_2$ (74%) and $Zr(H)_2(Cl)_2$ (58%) and has been rationalized in terms of maximal lowering of kinetic energy.[15]

The major effect of the phosphines here is to decrease the Pt d character (69–60%) and Pt s character (30% to 28%), to increase the Pt p character (1–12%), and to increase the charge transfer to the methyl (0.06–0.13 e^-). These changes arise because each phosphine lone pair forms a Lewis base/Lewis acid bond to the Pt by overlapping the empty valence s and p space of the metal atom. Thus, the $Mt(PH_3)_2$ complex favors the d^{10} configuration. However, with five doubly occupied d orbitals, the d^{10} configuration cannot form covalent bonds to CH_3 or H ligands. Thus, in order to add to H–H, H–C, or C–C bonds, the metal must be promoted from d^{10} to s^1d^9. With two singly occupied orbitals (one s and one d that may be hybridized to form two sd hybrids pointing at 90° to each other), the s^1d^9 state can form the requisite pair of covalent bonds. The singly occupied sd bonding orbitals must become orthogonal to phosphine lone pairs (not required for $Mt(CH_3)_2$), which they do by mixing in p character. This destabilization by the phosphines of the metal bonding orbitals makes them easier to ionize and thereby increases the ionic character of the M–C bonds.

Although Mulliken populations are always somewhat ambiguous in identifying the absolute location of charges (e.g., the dipole moment for PtH indicates that Pt is positively charged (Pt^+H^-)

(15) Steigerwald, M. L. Ph.D. Thesis, California Institute of Technology, 1984.

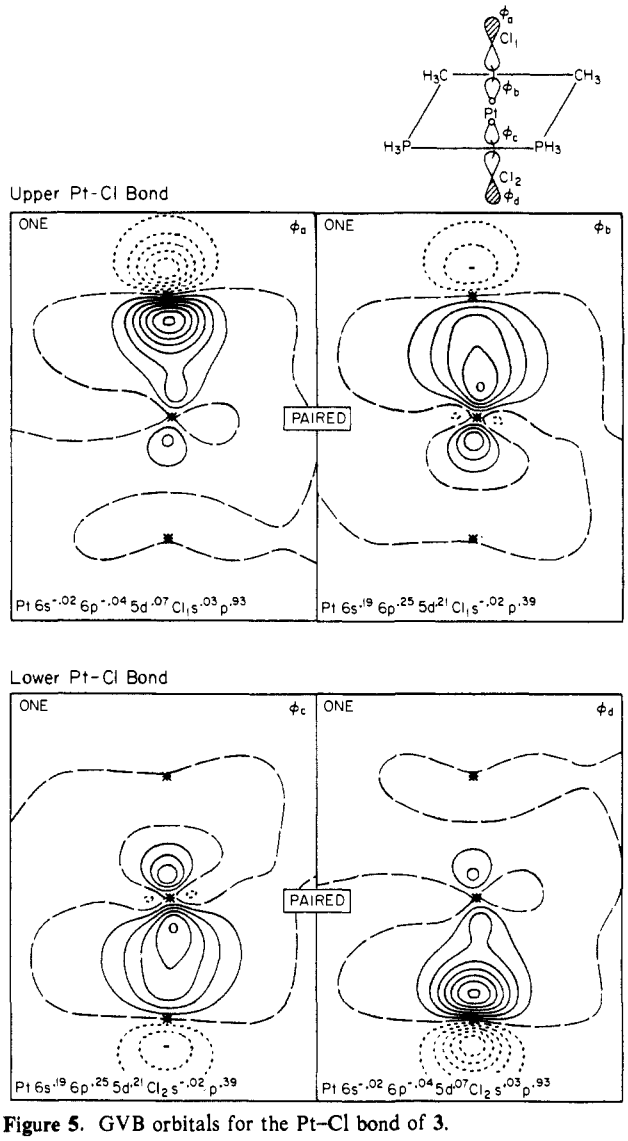

Figure 5. GVB orbitals for the Pt–Cl bond of **3**.

by an amount corresponding to a transfer of 0.26 e^- to H, whereas the Mulliken population indicates a positive charge on H of 0.1 e^-),[2a] we find these populations useful for comparisons with related systems. From Table II the total populations indicate that each phosphine in **1** is essentially neutral (−0.06 e^- total charge). The total populations on the Pt for **1** lead to $(sp)^{0.73}(d)^{8.89}$, reasonably consistent with the characterization as s^1d^9. The description of the two M–C bonds as covalent is in reasonable agreement with the Pauling electronegativities[16] (2.2 for Pt and 2.5 for C).

Changing the metal atom from Pt in **1** to Pd in **2** leads to a small increase in charge transfer to CH_3 (0.13 vs. 0.20 e^-) and to PH_3 (0.06 vs. 0.10 e^-), to a decrease in sp population (0.73 vs. 0.33 e^-), and to a slight increase in d population (8.89 vs. 9.09 e^-). These differences indicate that Pd has essentially the same electronegitivity as Pt (the Pauling scale assigns both as 2.2) and that Pd is biased toward d^{10} relative to s^1d^9. (This is expected since the ground state of the Pd atom is d^{10}, while that of Pt is s^1d^9.) The character of the GVB orbitals reflects these differences. Thus, when **1** (Pt) and **2** (Pd) are compared, the metal part of the Mt–CH_3 bond orbital has 0.17 vs. 0.24 e^- on the C, while the M sp character decreases by 0.09 e^- and the percentage d character on the metal part of the orbital increases from 60% to 67%.

Comparison of **1** and **4** allows us to analyze the differences between Pt–CH_3 and Pt–Cl bonds. The net effect of replacing both CH_3's by Cl is to decrease the charge on each PH_3 by 0.14

(16) Pauling, L. *The Nature of the Chemical Bond*, 3rd ed.; Cornell University Press: Ithaca, NY, 1960.

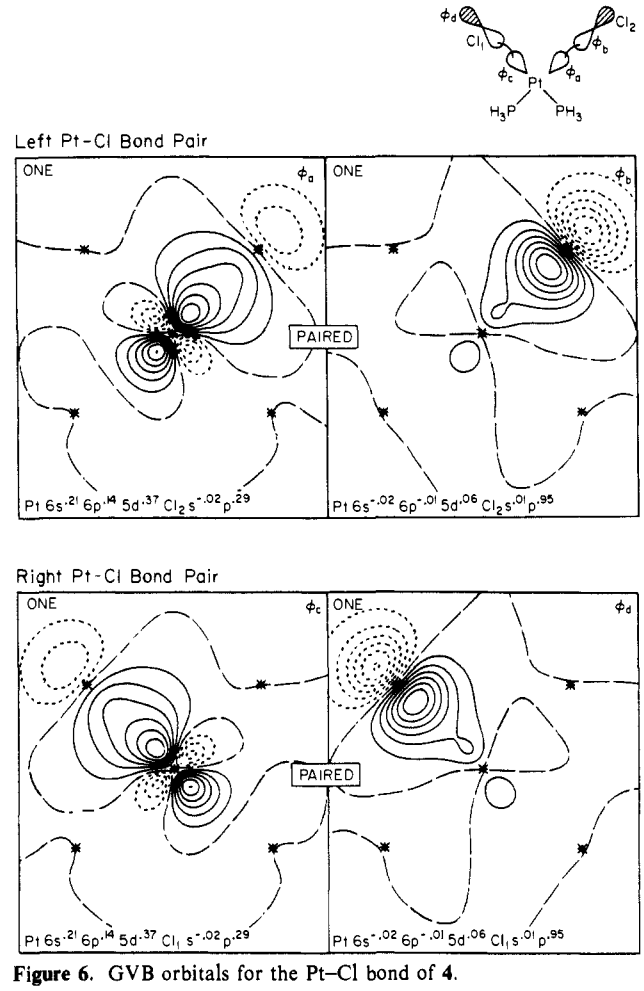

Figure 6. GVB orbitals for the Pt–Cl bond of **4**.

e^- and to decrease the charge on Pt by 0.07 e^-. Comparing the GVB orbitals, we see that the metal orbital is 27% on the Cl (vs. 17% on the CH_3) and that the percent d character of the metal part decreases from 60% to 51%. As would be expected, the Cl-like GVB orbital is nearly pure p character (95%) with very little metal character (3%).

In summary all complexes that would be described as Mt(II) in the normal oxidation state formalism are unoxidized and have s^1d^9 character on the metal. Thus, *oxidative addition* of these metals to H–H, H–C, and C–C bonds is *not oxidative*! In the GVB description, we think of the two singly occupied orbitals (s and d) as combined into sd hybrids (pointing at 90° from each other) and covalently paired with the singly occupied ligand orbital (H, CH_3, or Cl) to form a covalent bond pair. The presence of phosphines leads to destabilization of the M s orbital, with a concomitant increase in p character and increased charge transfer to the ligand. Thus, *we use the notation* Mt(II) *to indicate the configuration* (s^1d^9) *capable of forming* **two** *covalent bonds.*

2. Mt(IV) Systems. Before considering the Pt(IV) complex **3**, it is appropriate to examine the GVB description of the s^2d^8 state of Pt (as well as Ni and Pd). In the d^{10} state of Pt, the Hartree–Fock (HF) description has given doubly occupied valence orbitals, while the GVB description leads to five pairs of orbitals, each of which involves two overlapping orbitals of the same character (e.g., d_{xz}) orthogonal to the other four pairs. In each pair, one of these orbitals is more compact and the other is more diffuse (reflecting the tendency of the electrons to correlate their motions so as to reduce electron–electron interaction while keeping the electrons close to the nucleus). Thus, GVB describes d^{10} in terms of 10 orbitals for the 10 electrons, while HF uses 5 orbitals. However, since the GVB orbitals within each pair have a high overlap (S = 0.91) and similar shape, the GVB description leads to the same qualitative description as HF, and we discuss the d^{10} state as if there were five doubly occupied orbitals.

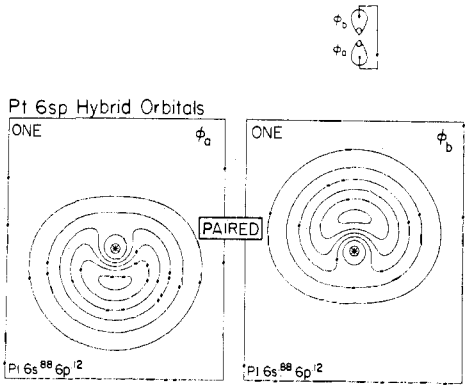

Figure 7. GVB orbitals for the s^2 pair of the d^8s^2 state of Pt.

For the s^1d^9 configuration, the ground state is ^3D, which in HF is described with four doubly occupied d orbitals, a singly occupied d orbital, and a singly occupied s orbital (a total of six). In the GVB description, each of the four doubly occupied HF orbitals leads to a pair of highly overlapping GVB orbitals so that GVB again as 10 orbitals for the 10 electrons. Although the shapes of the singly occupied orbitals change slightly between HF and GVB, there is again no qualitative difference in the description of the s^1d^9 state.

However, for s^2d^8, there *is* a qualitative difference between HF and GVB. Here the ground state is ^3F, leading in HF theory to three doubly occupied d orbitals, a doubly occupied s orbital, and two singly occupied d orbitals, for a total of six. In the GVB description there are once again 10 orbitals with three pairs of highly overlapping d orbitals (corresponding to the HF pairs), two singly occupied d orbitals, and a pair of orbitals corresponding to the HF s pair. However, this last pair of GVB orbitals differs remarkably from HF, leading to sp hybrids as shown in Figure 7. The overlap for this pair is 0.75, but most significantly these sp hybrids point to opposite sides of the atom so that they can *each participate in separate covalent bonds.* This is quite analogous to the situation in Zn, Cd, and Hg, where the valence s pair can make two covalent bonds (say to CH_3's), leading to a 180° bond angle. Indeed, the triplet state of PtH_2, $Pt(CH_3)_2$, and $PtCl_2$ should be linear, being formed by bonding to these sp hybrids, leaving a d^8 configuration (probably $^3\Delta$). (For Ni there should also be similar strongly bound triplet states; however, for Pd the very high energy of the s^2d^8 state may lead to unstable triplet states.) Of course the two singly occupied d orbitals can also be used for bonding, leading to a total of *four* possible covalent bonds for Pt s^2d^8. Electronegative ligands favor bonding to the sp hybrid orbital[17] since the ionization potential of the s orbital is 2.79 eV lower (leading to Pt^+ s^1d^8) than the d orbital (leading to Pt^+ s^2d^7). Thus, in **3** we expect the Pt–Cl bonding to favor Pt sp, while Pt–CH_3 should favor Pt d. In addition, bonding both Cl to sp orbitals should favor trans Cl ligands.

Indeed, the geometry of **3** is essentially octahedral (vide infra). (We have assumed the Cl as trans and the CH_3 groups as cis.) Comparing the Mt–Cl bonds in **4** and **3**, we see an increase in ionic character for **3** (for the metal-like orbital the number of electrons on the Cl increases from 0.27 to 0.37 e^-). Concomitantly, the d character on the metal part of the metal orbital decreases from 52% to 32%, while the ratio of p to s increases from 2/3 to 4/3. Comparing the Mulliken populations in **1** and **3**, we see a slight change in polarity from Pt^+C^- to Pt^-C^+, while remaining essentially covalent (the Pt component of the metal orbital increases from 0.82 to 0.93 e^-, while the component of C character of the methyl orbital decreases from 0.89 to 0.78 e^-). Simultaneously, the d character in the metal part of the bond pair increases dramatically (60–74%), as expected.

To simplify the description we will refer to the Pt–C bond in **3** as a *covalent* bond to a Pt 5d orbital and the Pt–Cl bond as a *partially ionic* bond to a Pt 6sp hybrid orbital. In this simplified picture we visually represent the Pt(IV) complexes as having the Pt atom promoted to the s^2d^8 configuration, having two sp hybrid pairs as in Mg, Al, and Si.

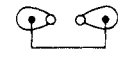

9

This state is the only one that can allow the Pt atom to form four covalent bonds: two bonds to singly occupied d orbitals and two bonds to the pair of sp lobe orbitals.[18]

The Mulliken populations for **3** are ambiguous in assigning the electronic configuration of the Pt atom. Significant amounts of charge transfer from the Pt sp orbitals to the chlorines (0.56 e^-) and from the methyl groups to the Pt d orbitals (0.28 e^-) make the Pt atom appear intermediate between s^2d^8 and s^1d^9 (8.33 e^- in d orbitals and 1.12 e^- in s and p orbitals). Adjusting the Mulliken populations by assigning the excess charge on the chlorines as Pt sp and replacing the charge deficiency on the methyl groups with charge from the Pt $d\pi$ orbitals, we obtain a charge of 1.68 for sp and 8.05 for d, reasonably close to s^2d^8.

The bonding in this Pt(IV) complex is essentially covalent, which should not be too surprising since the Pauling electronegatively[16] for Pt is 2.2 vs. 3.0 for Cl and 2.5 for carbon.

3. Mt(0) Systems. The ground state of Pd(0) is d^{10}, with the (triplet) s^1d^9 configuration 21.9 kcal/mol higher[18] (calculated value 19.6 kcal/mol). The ground state of Pt is s^1d^9 with the d^{10} state 11.0 kcal/mol higher[18] (calculated value 12.3 kcal/mol). For both Pd and Pt, reductive coupling involves s^1d^9 for the reactant and d^{10} for the product, and hence reductive coupling should be more exothermic for Pd than for Pt by 21.9 + 11.0 = 32.9 kcal/mol (calculated value 31.9 kcal).

The lowest *singlet* state of Pt(0) is d^{10} so that the spin-allowed product of

$$Mt(R_1)(R_2) \rightarrow Mt + R_1\text{–}R_2 \qquad (6)$$

is d^{10} in both cases. Adding two phosphines stabilizes d^{10} with respect to s^1d^9 so that the ground state of $Mt(PH_3)_2$ is the linear d^{10} singlet for both Mt = Pd and Pt. This stabilization of d^{10} arises from overlap between the phosphine lone pair and the metal valence s orbital. If the Mt s orbital is empty (d^{10}), the phosphine lone pair can donate into this orbital (Lewis base/Lewis acid interaction), leading to extra bonding. If the metal s orbital is occupied, it must be orthogonalized to the phosphine lone pair, increasing the energy. The result is that reductive coupling from $Mt(Ph_3)_2$ is about 20–25 kcal/mol more exothermic for both Mt = Pd and Pt.

4. Summary. Our conclusion is that the oxidation-state formalism for Pt and Pd complexes should be interpreted in terms of *maximum covalency rather than the degree of oxidation.* Thus, Pt(II) and Pd(II) should be considered as *neutral* atoms with a s^1d^9 configuration, forming *two* covalent bonds, while Pt(IV) should be described as a neutral platinum atom in an s^2d^8 configuration, forming *four* covalent bonds. We will find this view to be quite useful in rationalizing the relative reaction energetics of Pt(II) vs. Pd(II) and of Pt(II) vs. Pt(IV) (section II.C), where appropriate atomic excitation energies provide excellent predictions.

B. Energetics. The energetics for various reactions were obtained by calculating GVB correlated wave functions (which give accurate s^1d^9–d^{10} state splittings) at geometries optimized for HF wave functions (see section IV for calculational details). The results are summarized in Table III.

1. Calculated Energetics for C–C Reductive Coupling. Considering C–C coupling processes, we find

$$Pt(CH_3)_2(PH_3)_2 \rightarrow Pt(PH_3)_2 + C_2H_6 \qquad (7)$$

$$\Delta H_7 = -11.3 \text{ kcal/mol}$$

(17) A similar preference for p vs. s character is found in carbon–halogen bonds. Goddard, W. A., III; Hardling, L. B. *Annu. Rev. Phys. Chem.* **1979**, *29*, 363–396.

(18) Moore, C. E. *Atomic Energy Levels*; National Bureau of Standards: Washington, DC, 1971; Vol. III. (These state splittings were averaged over *j* states to cancel out spin-orbit coupling.)

Table III. Calculated and Predicted Energetics for Reductive Coupling Processes[a]

	$M(H)_2 \rightarrow M + H_2$				$M(H)(CH_3) \rightarrow M + CH_4$			$M(CH_3)_2 \rightarrow M + C_2H_6$			
	ΔE	ΔH_{298}	$\Delta E^{\ddagger}$	$\Delta H^{\ddagger}$	ΔE	ΔH_{289}	$\Delta E^{\ddagger}$	$\Delta H^{\ddagger}$	ΔE	ΔH_{298}	$\Delta E_{\ddagger}$	$\Delta H_{\ddagger}$
(a) M = Pt	33.6	33.2	*b*	*b*	16.1	19.0	29.0	28.1	18.3	15.5	53.5	54.5
M = $Pt(PH_3)_2$	15.9	12.3	18.1	14.0	−7.2	−5.8	(17.3)	(15.7)	−8.1	−11.3	(40.3)	(41.1)
PH_3 destabilization	17.7	20.9			23.3	24.8	(11.7)	(12.4)	26.4	26.8	(13.2)	(13.4)
(b) M = Pd	−3.6	−4.0	1.6	0.4	−20.1	−17.2	10.4	9.5	−16.0	−18.8	22.6	23.6
M = $Pd(PH_3)_2$	(−21.5)	(−25.1)	((−7.4))[c]	((−10.2))[c]	(−43.6)	(−42.2)	((−1.4))[c]	((−3.0))[c]	−42.6	−45.8	(9.3)	(10.1)
PH_3 destabilization	(17.9)	(21.1)	((9.0))	((10.6))	(23.5)	(25.0)	((11.8))	((12.5))	26.6	27.0	(13.3)	(13.5)
(c) M = $Pt(Cl)_2(PH_3)_2$	(7.7)	(2.5)	((14.0))	((9.1))	(−22.0)	(−19.5)	((10.4))	((8.8))	−25.0	−27.0	(31.8)	(34.2)
Cl destabilization	(8.2)	(9.8)	((4.1))	((4.9))	(13.8)	(13.7)	((6.9))	((6.9))	16.9	15.7	(8.5)	(7.9)
(d) M = $Pd(Cl)_2(PH_3)_2$	((−37.7))[d]		(((−15.5)))[c]		((−67.4))[d]		(((−13.3)))[c]		(−70.4)[d]		((−4.6))[c]	
Cl destabilization	((16.2))		(((8.1)))		((23.8))		(((11.9)))		(27.8)		((13.9))	

[a] All energies are in kcal/mol. ΔH_{298} is the reaction enthalpy at 298 K, which is obtained from the calculated energy difference (ΔE) by adding in estd. zero-point energy and temperature corrections. $\Delta E^{\ddagger}$ is the calculated energy barrier for reductive coupling, and $\Delta H^{\ddagger}$ is the predicted activation barrier at 298 K. Parentheses indicate the level of approximation in obtaining an estimated value. Each level of parentheses probably adds an additional uncertainty of ±5 kcal/mol. [b] No barrier is found for oxidative addition. [c] No barrier is found for reductive coupling. The negative values indicate the estimated energy (relative to the product) at the geometry corresponding to the transition state for $Mt(R_1)(R_2) \rightarrow Mt + R_1 - R_2$. [d] Based on correcting the M = $Pt(Cl)_2(PH_3)_2$ case using ΔE = 45.4 kcal/mol ($Pt(d^9s^1 \rightarrow d^8s^2)$ = 17.2 kcal/mol and $Pd(d^9s^1 \rightarrow d^8s^2)$ = 62.6 kcal/mol).

which can be compared to

$$Pt(CH_3)_2 \rightarrow Pt + C_2H_6 \quad (8)$$

$$\Delta H_8 = 15.5 \text{ kcal/mol}$$

Thus, the presence of two phosphines favors reductive coupling by an extra 26.8 kcal/mol. The reason for this is that the Pt has a s^1d^9 configuration for the reactant side of (7) and (8) but a d^{10} configuration for the product side. As discussed in section II.A.3, phosphines stabilize d^{10} relative to s^1d^9, leading to a more exothermic reaction.

Consider next the analogous reactions with Pd,

$$Pd(CH_3)_2(PH_3)_2 \rightarrow Pd(PH_3)_2 + C_2H_6 \quad (9)$$

$$\Delta H_9 = -45.8 \text{ kcal/mol}$$

which can be compared to

$$Pd(CH_3)_2 \rightarrow Pd + C_2H_6 \quad (10)$$

$$\Delta H_{10} = -18.8 \text{ kcal/mol}$$

The reaction enthalpies differ dramatically from those of Pt; however, these differences are easily explained. All four reactions involve converting the metal from s^1d^9 to d^{10}, but using d^{10} as the reference Pt *favors* s^1d^9 by 12.3 kcal/mol, whereas Pd *disfavors* s^1d^9 by 19.6 kcal/mol. Thus, relative to Pt, Pd has a bias against s^1d^9 of 31.9 kcal/mol. Consequently, the driving force for Pd reductive coupling should be exothermic by 31.9 kcal/mol more than for Pt. Indeed, we calculate a difference of 34.5 kcal/mol for the bis(phosphine) and 34.3 kcal/mol for the unsubstituted metal.

These results for Mt(II) can be compared to the Mt(IV) reaction,

$$Pt(CH_3)_2(Cl)_2(PH_3)_2 \rightarrow Pt(Cl)_2(PH_3)_2 + C_2H_6 \quad (11)$$

$$\Delta H_{11} = -27.0 \text{ kcal/mol}$$

Here the metal changes from s^2d^8 to s^1d^9, which for the free atom is exothermic by 17.2 kcal/mol. Comparing to (7) which involves s^1d^9 to d^{10}, which is endothermic in the atom by 12.3 kcal/mol, we would expect from atomic considerations that (11) should be 29.5 kcal/mol more exothermic than (7). Of course the four-coordinate Pt(II) and six-coordinate Pt(IV) also differ in other respects; however, we find that (11) is 16 kcal/mol more exothermic than (7), so that the atomic change of configuration effects dominate.

On the basis of differential atomic excitation energies, the Pd analogue of (11) should be exothermic by an extra 45 kcal/mol, leading to a total exothermicity (ΔE) of about 70 kcal/mol. We estimate that there is no barrier for this decomposition and hence that this species is unstable.

Summarizing, we find that reductive CC coupling is exothermic by 45.8 kcal/mol for Pd(II), by 27.0 kcal/mol for Pt(IV), and by 11.3 kcal/mol for Pt(II), differences that can be understood in terms of the relative atomic energies of s^1d^9, d^{10}, and s^2d^8 configurations.

2. Calculated Energetics for C–H Reductive Coupling. We calculate that

$$Pt(H)(CH_3)(PH_3)_2 \rightarrow Pt(PH_3)_2 + CH_4 \quad (12)$$

$$\Delta H_{12} = -5.8 \text{ kcal/mol}$$

whereas

$$Pt(H)(CH_3) \rightarrow Pt + CH_4 \quad (13)$$

$$\Delta H_{13} = 19.0 \text{ kcal/mol}$$

Thus, two phosphines promote H–C reductive coupling by 24.8 kcal/mol, which can be compared with a promotion of 26.8 kcal/mol for C–C reductive coupling on Pt and 27.0 for C–C reductive coupling on Pd. For Pd we studied reductive coupling for the free atoms, finding

$$Pd(H)(CH_3) \rightarrow Pd + CH_4 \quad (14)$$

$$\Delta H_{14} = -17.2 \text{ kcal/mol}$$

Table IV. Average Bond Energies for $M(R_2)$ Complexes (kcal/mol)

molecule	excitation energy	M–H		M–CH_3		difference in M–H and M–CH_3 bond energies
		$\bar{D}_{298}$	D_1	$\bar{D}_{298}$	D_1	
M = Pt	−12.3	68.7	62.6	53.0	46.9	15.7
M = Pd	+19.6	50.1	59.9	35.8	45.7	14.2
M = $Pt(PH_3)_2$	+32.1[a]	58.3	(74.4)	39.6	55.7	18.7
M = $Pd(PH_3)_2$	+57.2[a]	(39.6)	(68.2)	22.3	50.9	(17.3)
M = $Pt(Cl)_2(PH_3)_2$	38.6[a]	(53.4)	(72.7)	31.7	51.0	(21.7)
M = $Pd(Cl)_2(PH_3)_2$	(84.0)[b]	((33.3))	((75.3))	(10.0)	(52.0)	((23.3))

[a] Based on the geometry of the $M(CH_3)_2$ complex. [b] Based on ΔE = 38.6 kcal for the Pt complex plus the differential d^9s^1 to d^8s^2 energy (45.4 kcal).

but did not calculate the H–C coupling from the bis(phosphine). However, the above results suggest that for Pd the bis(phosphine) would promote H–C reductive coupling by ~25.0 kcal/mol, leading to

$$Pd(H)(CH_3)(PH_3)_2 \rightarrow Pd(PH_3)_2 + CH_4 \quad (15)$$

$$\Delta H_{15} \approx -42.2 \text{ kcal/mol}$$

We did not calculate the energetics for H–C coupling from Pt(IV) or Pd(IV) complexes; however, comparisons with the C–C coupling cases suggest that

$$Pt(H)(CH_3)(Cl)_2(PH_3)_2 \rightarrow Pt(Cl)_2(PH_3)_2 + CH_4 \quad (16)$$

$$\Delta H_{16} \approx -19.5 \text{ kcal/mol}$$

while the analogous Pd complex would not be stable.

3. Calculated Energetics for H–H Reductive Coupling. We calculate that

$$Pt(H)_2(PH_3)_2 \rightarrow Pt(PH_3)_2 + H_2 \quad (17)$$

$$\Delta H_{17} = 12.3 \text{ kcal/mol}$$

whereas

$$Pt(H)_2 \rightarrow Pt + H_2 \quad (18)$$

$$\Delta H_{18} = 33.2 \text{ kcal/mol}$$

Thus, the phosphines promote H–H reductive coupling by 20.9 kcal/mol, which can be compared with 24.8 kcal/mol for H–C and 26.8 kcal/mol for C–C. For Pd we studied reductive coupling from the free atom, finding

$$Pd(H)_2 \rightarrow Pd + H_2 \quad (19)$$

$$\Delta H_{19} = -4.0 \text{ kcal/mol}$$

but did not calculate the reductive H–H coupling from the bis(phosphine). However, the above results suggest that the phosphines would promote H–H coupling on Pd by about 21.1 kcal/mol, leading to

$$Pd(H)_2(PH_3)_2 \rightarrow Pd(PH_3)_2 + H_2 \quad (20)$$

$$\Delta H_{20} \approx -25 \text{ kcal/mol}$$

We did not calculate the energetics of H–H coupling from Pt(IV) or Pd(IV) complexes; however, we estimate that

$$Pt(H)_2(Cl)_2(PH_3)_2 \rightarrow Pt(Cl)_2(PH_3)_2 + H_2 \quad (21)$$

$$\Delta H_{21} \approx 2.5 \text{ kcal/mol}$$

and that the analogous Pd complex is unstable.

4. Adiabatic Bond Energies. Since the C–C bond energy in ethane is 90.4 kcal/mol,[19] the exothermicity of 11.3 kcal/mol for (7) leads to an average Pt–C bond energy of

$$D_{298}[(PH_3)_2Pt\text{–}CH_3] = 39.6 \text{ kcal/mol} \quad (22)$$

Similarly, since the H–H bond energy is 104.2 kcal/mol,[19a] the energetics in (17) correspond to an average Pt–H bond energy of

$$\bar{D}_{298}[(PH_3)_2Pt\text{–}H] = 58.3 \text{ kcal/mol} \quad (23)$$

As a check upon the utility of such average bond energies, we can use (22) and (23) plus the C–H bond energy in CH_4 (105.1 kcal/mol)[19b] to predict

$$\Delta H_{12} = 39.6 + 58.3 - 105.1 = -7.2 \text{ kcal/mol}$$

in reasonable agreement with the calculated value of −5.8 kcal/mol.

The average bond energies for the bare metal are obtained from (8) and (18) as

$$\bar{D}_{298}(Pt\text{–}CH_3) = 53.0 \text{ kcal/mol} \quad (24)$$

$$\bar{D}_{298}(Pt\text{–}H) = 68.7 \text{ kcal/mol} \quad (25)$$

which leads to a prediction of

$$\Delta H_{13} = 53.0 + 68.9 - 105.2 = +16.5 \text{ kcal/mol}$$

in reasonable agreement with the calculated value of ΔH_{13} = 19.0 kcal/mol.

The average bond energies for Pd complexes are calculated to be about 18 kcal/mol lower (see Table IV) because of the propensity for Pd to form d^{10} configurations.

Averaging the results for Pd and Pt, we find that M–H bonds are 18 kcal/mol stronger than M–CH_3 bonds for the bis(phosphine) and 15 kcal/mol stronger for the bare metal. Thus, the phosphines lead to a relative weakening of M–CH_3 vs. M–H bonds. This could be simply a steric effect. If so, the bulky phosphines endemic to experiments might have even a greater bias against M–CH_3 bonds.

The Pt(IV) system leads to weaker Pt–CH_3 bonds,

$$\bar{D}_{298}[(Cl)_2(PH_3)_2Pt\text{–}CH_3] = 31.7 \text{ kcal/mol} \quad (26)$$

As discussed above, this 8 kcal/mol decrease from the value for Pt(II) is dominated by the preference of Pt convert from s^2d^8 to d^9s^1.

5. Intrinsic Bond Energies. It is often useful to define an *intrinsic bond strength* as the energy to break a bond A–B *without* allowing the fragments to relax. This intrinsic bond strength is then reduced by various relaxation effects that occur in the fragments A and B after the bond is broken. These relaxation effects can involve *geometric relaxation* and *electronic relaxation*. The final bond energy including all these effects is the adiabatic bond energy $\bar{D}_{298}$. Thus, for example, the C–H bond energy of cyclopropane is 11 kcal/mol stronger[20] than for H–$CH(CH_3)_2$ partly because geometric constraints prevent most of the geometry relaxation in cyclopropane.

A good example for the role of electronic relaxation upon bond energy is in the difference in carbon–carbon double bond strengths in C_2H_4 and C_2F_4.[21] The double bond requires a singly occupied σ and π orbital on each carbon corresponding to the $^3B_1$ state of free CH_2 or CF_2. For CH_2, the triplet state is the ground state and hence the observed (adiabatic) bond energy of 172.2 kcal/mol[22] is electronically diabatic (it involves a small amount of

(19) The D_{298} used in these calculations are D_{298}(H–H) = 104.2 kcal/mol, D_{298}(H–CH_3) = 105.1 kcal/mol, and D_{298}(H_3C–CH_3) = 90.4 kcal/mol. These bond energies were derived from spectroscopic measurements of H_2[19a] and the reported D_{298}[19b] for H_3C–CH_3 and H–CH_3. (a) Huber, K. P.; Herzberg, G. *Constants of Diatomic Molecules*; Van Nostrand: New York, 1979. (b) McMillen, D. F.; Golden, D. M. *Annu. Rev. Phys. Chem.* **1982**, *33*, 493–352.

(20) D_{298}[cyclopropyl-H] = 106.3 kcal/mol;[16b] D_{298}[H–$CH(CH_3)_2$] = 95.1 kcal/mol.[16b]

(21) Simons, J. P. *Nature (London)* **1965**, *205*, 1308–1309; Carter, E. A.; Goddard, W. A., III *J. Phys. Chem.* **1986**, *90*, 998–1001.

geometric relaxation). However, for CF_2, the $^3B_1$ state is 56.6 kcal/mol[23] above the ground state ($^1A_1$). Thus, if the diabatic C–C double bond energy is assumed unchanged (172.2 kcal/mol), we would expect the adiabatic bond energy in C_2F_4 to be 172.2 − 2(56.6) = 59.0 kcal/mol. This is in good agreement with the observed bond energy of 69.0 ± 2.7 kcal/mol,[22] demonstrating the power in using the concept of electronic relaxation in estimating bond energies.

The adiabatic bond energies calculated in the previous section included both geometrical and electronic relaxation effects. In order to correct the average bond energies for these relaxation effects, we must add the atomic excitation energy ($d^{10} \rightarrow d^9s^1$ or $s^1d^9 \rightarrow s^2d^8$) in the complex to the driving force for reductive elimination. We calculate the energy of the triplet at the geometry of the $Mt(PH_3)_2$ (or $MtCl_2(PH_3)_2$) fragment in the $MtR_2(PH_3)_2$ (or $MtR_2Cl_2(PH_3)_2$) complex. Of course the energy of the $Mt(PH_3)_2$ (or $MtCl_2(PH_3)_2$) singlet was calculated at the equilibrium geometry. The singlet–triplet splittings calculated with these reference states include all differential relaxation effects which occur during reductive elimination from these complexes. Thus, the *intrinsic bond energy* is defined as

$$D_1 = \tfrac{1}{2}[\Delta H(\bar{M}R_2 \rightarrow M + R_2) + \delta E(M \rightarrow \bar{M}) + D_{298}(R\text{–}R)] \quad (27)$$

where $\delta E(M \rightarrow \bar{M})$ is the singlet–triplet excitation energy described above, M is the singlet metal complex product in its ground-state geometry, and $\bar{M}$ is the triplet state of the same complex frozen at the geometry it had in the reactant complex.

Average bond energies and the relevant state splittings are presented in Table IV. The corrected bond energies show that the *intrinsic* strengths of Pt–C and Pd–C bonds are very similar and that the relative stability toward reductive coupling is dominated by the relative energies of the s^1d^9 and d^{10} states and of bent vs. linear phosphines. Comparing the intrinsic Mt–R bond strengths of bis(phosphine) complexes (e.g., 56 kcal/mol for $Pt(CH_3)_2(PH_3)_2$) and the corresponding MtR_2 complexes[2c] (e.g., 47 kcal/mol for $PtMe_2$) indicates that the presence of phosphines strengthens the intrinsic Mt–R bonds by 6–12 kcal/mol. This is because the metal spd hybrid orbitals used to form the M–R bonds must be orthogonalized to the phosphines, leading to an increase in the p character of the metal hybrid. This in turn increases the overlap of the M–R bond,[15] increasing the intrinsic bond strength. On the other hand, the phosphines lead to a decrease in the adiabatic bond energies (from 53 kcal/mol for $Pt(CH_3)_2$ to 40 kcal/mol for $Pt(CH_3)_2(PH_3)_2$). This is probably because the phosphines greatly favor the d^{10} form of the product.

The intrinsic Pt^{IV}–C bond is 5 kcal/mol weaker than the Pt^{II}–C bond in bis(phosphine) complexes. This is probably because the Pt 6s character of the Pt^{IV}–C bonds is used up in the Pt–Cl bonds. Consequently, the methyl group in Pt(IV) is forced to bond to metal orbitals that have mainly d character rather than the optimal hybridization[15] (~60% d and 40% sp) that is available in the platinum(II) bis(phosphine) complex.

Few bond strengths are known experimentally for Pt–C or Pd–C. From studies of the decomposition of $PtMe_3Cp$,[24] an experimental Pt–CH_3 bond energy of 39 ± 5 kcal/mol has been determined. This is an adiabatic bond energy,

$$PtMe_3Cp \rightarrow {}^{\bullet}Me + {}^{\bullet}PtMe_2Cp \quad (28)$$

but the Pt atom no doubt retains s^2d^8 character. Thus, the exothermicity of (28) should be less than the intrinsic bond energy (51 kcal/mol) but probably larger than our estimated adiabatic bond strength of 32 kcal/mol, which involves relaxation to s^1d^9. Thus, the theory and experiment are in reasonable agreement.

C. **Barriers and Rates.** In previous studies of[2]

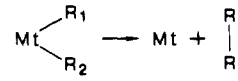

(29)

where Mt = Pd or Pt and R_1 or R_2 = H or CH_3, we showed that the *intrinsic barrier* (i.e., the barrier exceeding the endothermicity) is (i) large for CC coupling (e.g., 23 kcal/mol for Pd, 54 kcal/mol for Pt), (ii) intermediate for CH coupling (e.g., 10 kcal/mol for Pd, 29 kcal/mol for Pt), and (iii) small for HH coupling (e.g., 2 kcal/mol for Pd). The origin for such dramatic differences for H–H, H–C, and C–C coupling is found in the shapes of the H 1s and C sp^3 orbitals. At the transition state, the wave function involves a mixture of the s^1d^9 resonance structure **10** for the reactant

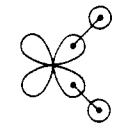

10

and the d^{10} resonance structure **11** of the product

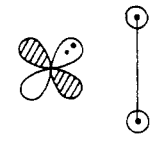

11

Since the H 1s orbital is spherical, it can simultaneously overlap either the Mt sd hybrid orbital in **10** or the valence orbital of the other R group in **11**. The result is that these two resonance structures have a high overlap for $R_1 = R_2 = H$, leading to a large resonance stabilization and a low barrier. If $R_1 = H$ and $R_2 = CH_3$, then the directed form of the valence orbital for CH_3 is such that one CH_3 orientation favors **10**

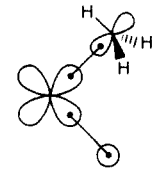

12

while a *different* CH_3 orientation favors **11**

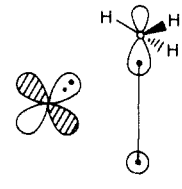

13

Consequently, at the transition state the CH_3 group has an intermediate orientation which is less favorable for both **10** and **11**, leading to a significant barrier. If $R_1 = R_2 = CH_3$, then there is a similar problem for *both* ligands, leading to a barrier that is roughly twice as large.

Adding two phosphines to the metal stabilizes the d^{10} state over s^1d^9, making reductive coupling about 23 kcal/mol more exothermic (27 kcal/mol for H–H, 23 kcal/mol for H–C, and 21 kcal/mol for C–C) and should similarly decrease the activation barrier. Assuming that the transition state involves about equal

(22) $D_{298}[H_2C{=}CH_2]$ = 172.2 ± 2.07 kcal/mol and $D_{298}[F_2C{=}CF_2]$ = 69.3 ± 2.7 were derived from the following enthalpies: $\Delta H_f(C_2F_4)$ = −157.7 ± 0.7 kcal/mol (see: Stull, D. R.; Prophet, H. *JANAF Thermochemical Tables*, 2nd ed.; National Bureau of Standards: Washington, DC, June 1971; NSRDS-NBS 37), $\Delta H_f(C_2H_4)$ = 12.54 ± 0.07 kcal/mol (see: Stull, D. R.; Prophet, H. *JANAF Thermochemical Tables*, 2nd ed.; National Bureau of Standards: Washington, DC, June 1971; NSRDS-NBS 37), $\Delta H_f(CH_2)$ = 92.35 ± 1.0 kcal/mol (Chase, M. W.; Curnett, J. L.; Prophet, H.; McDonald, R. A.; Syverd, A. N. *J. Phys. Chem. Ref. Data* **1975**, *4*, 1–175), and $\Delta H_f(CF_2)$ = −44.2 ± 1.0 kcal/mol (Berman, D. W.; Bomse, D. S.; Beauchamp, J. L. *Int. J. Mass Spectrom. Ion Phys.* **1981**, *39*, 263–271).

(23) (a) Koda, S. *Chem. Phys. Lett.* **1978**, *55*, 353–357; *Chem. Phys.* **1982**, *66*, 383–390. (b) A theoretical calculation leads to 51.4 kcal/mol: Feller, D.; Borden, W. T.; Davidson, E. R. *Chem. Phys. Lett.* **1980**, *71*, 22–26.

(24) Egger, K. W. *J. Organomet. Chem.* **1970**, *24*, 501–506.

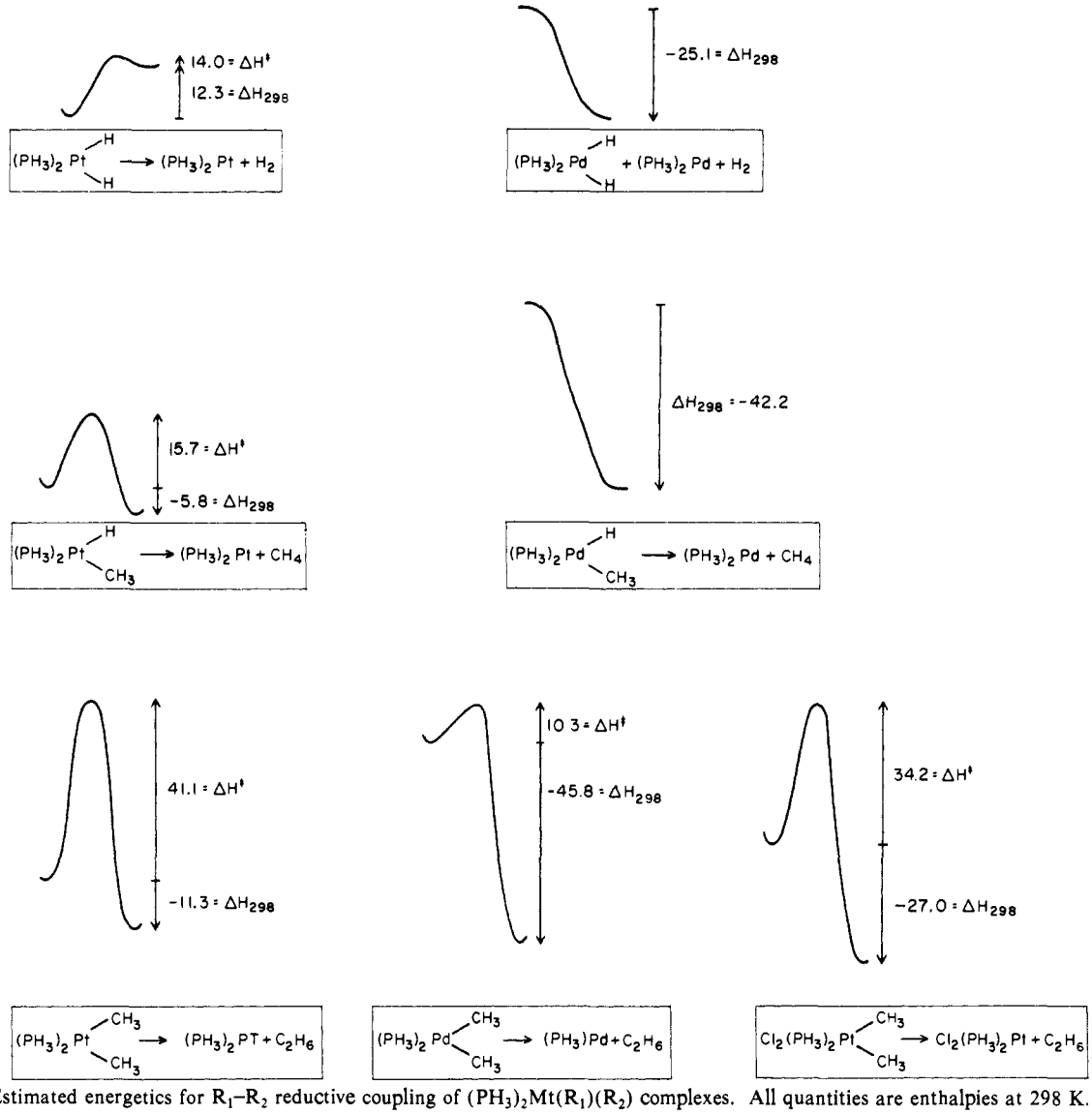

Figure 8. Estimated energetics for R_1–R_2 reductive coupling of $(PH_3)_2Mt(R_1)(R_2)$ complexes. All quantities are enthalpies at 298 K.

parts of the d^{10} and s^1d^9 configurations, it is plausible that the barrier will be decreased by about half as much as is the reactive enthalpy. This leads to the estimated activation energies in Table III and Figure 8.

Particularly clean experiments have been carried out for H–C coupling from Pt(II),[12,13] (12), for which we estimate $\Delta H^{\ddagger}_{12}$ = 15.7 kcal/mol. This can be compared to

$$cis\text{-}Pt(H)(CH_2CF_3)(PPh_3)_2 \rightarrow Pt(PPh_3)_2 + CH_3CF_3 \qquad (30)$$

where in benzene solvents $\Delta H^{\ddagger}$ = 24.6 ± 0.6 and $\Delta S^{\ddagger}$ = 4.9 ± 2.0, and to

$$cis\text{-}Pt(H)(CH_3)(PPh_3)_2 \rightarrow Pt(PPh_3)_2 + CH_4 \qquad (31)$$

where (in toluene at −25 °C) $\Delta G^{\ddagger}$ = 18.2.[12] Assuming $\Delta S^{\ddagger} \approx$ 5, this latter value leads to $\Delta H^{\ddagger}$ = 17.0 kcal/mol, in good agreement with our predictions.

Other relevant activation energies have been measured by Moravskiy and Stille[6c] for reductive elimination of ethane from *cis*-$Pd(CH_3)_2(PPh_2(CH_3))_2$. They find activation energies (E_a) of 6–11 kcal/mol in polar-coordinating solvents (Me_2SO-d_6, Me_2CO-d_6, and CD_3CN) and 25–28 kcal/mol in aromatic solvents ($C_6D_5CD_3$ and C_6D_6). It is uncertain how to compare these numbers with our calculations since it is likely that reductive elimination does not proceed directly from the bis(phosphine) complex (see section III.A). However, we estimate $\Delta H^{\ddagger}_9$ = 10.4 kcal/mol (at 300 K), and hence the estimated barrier (at 300 K) is $E_a = \Delta H^{\ddagger} + RT$ = 10.7 kcal/mol, surprisingly close to the E_a measured in coordinating solvent.

On the other hand, our estimates lead to $\Delta H^{\ddagger}_7$ = 41 kcal/mol for C–C coupling on Pt(II), certainly consistent with the lack of observation of this reaction.

The calculated endothermicity (ΔH_{17} = 12.3 kcal/mol) and barrier ($\Delta H^{\ddagger}_{19}$ = 14.0 kcal/mol) for H–H coupling from Pt(II) are consistent with the equilibrium observed in such systems by Trogler.[14] On the other hand, our calculations suggest that *cis*-$Pd(H)_2(PH_3)_2$ and *cis*-$Pd(H)(CH_3)(PH_3)_2$ would have no barrier for decomposition and hence should not be stable.

The estimated barriers for Mt(IV) complexes are much more uncertain since barriers were not calculated even for complexes without phosphines. In this case we have assumed that half of the addition exothermicity relative to Mt(II) goes into the transition state.

Brown et al.[7b] have measured E_a for the reductive elimination of ethane from various Pt(IV) trimethyl complexes. They find E_a = 27.7 ± 1.2 for reductive elimination from $PtCl(CH_3)_3(PMe_2Ph)_2$ at 353 K. Our estimate is E_a = 34.9 kcal/mol ($\Delta H^{\ddagger}_{11}$ = 34.2 kcal/mol) for elimination from $PtCl_2(CH_3)_2(PH_3)_2$. The good agreement between experiment and theory may be fortuitous since it appears experimentally that the reductive elimination takes place from a five-coordinate intermediate formed by loss of phosphine. Similar estimates for H–H and H–C coupling from Pt(IV) lead to $\Delta H^{\ddagger}$ = 9 kcal/mol for both reactions, indicating rather unstable species. The analogous Pd(IV) complexes are predicted to be unstable.

Experimentally it is known that Pt(II) dimethyl complexes are much more stable than Pd(II) dimethyl complexes, with C–C

Table V. Geometric Parameters around the Metal Atom in Pt and Pd Complexes (All Distances Are in Å and All Angles Are in deg)

molecule	distances			angles		
	M-P	M-C	misc.	P-M-P	C-M-C	misc.
1, $Pt(CH_3)_2(PH_3)_2$	2.46	2.06		101	89	
2, $Pd(CH_3)_2(PH_3)_2$	2.50	2.02		98	81	
3, $PtCl_2(CH_3)_2(PH_3)_2$	2.44	2.03	M-Cl (2.38)	95	90	Cl-M-Cl (177)
4, $PtCl_2(PH_3)_2$	2.44		M-Cl (2.35)	102		Cl-M-C (97)
5, $Pt(H)(CH_3)(PH_3)_2$[a]	2.46	2.06	M-H (1.50)	101		H-Pt-O (84)
6, $PtH_2(PH_3)_2$[b]	2.45		M-H (1.50)	100		H-Pt-H (79)
7, $Pt(PH_3)_2$	2.32			180		
8, $Pd(PH_3)_2$	2.41			180		
$Pt(CH_3)_2$[c]		1.97			98	
$Pt(H)(CH_3)$[c]		1.96	M-H (1.48)			H-Pt-C (98))
$Pt(H)_2$[c]			M-H (1.51)		83	
$Pd(CH_3)_2$[c]		1.96			92	

[a] This geometry was not optimized but was estimated from the geometries **1** and **6**. The geometries of the $Pt(CH_3)(PH_3)$ fragment were taken frozen at the geometry of **1**, and the C-Pt-H angle was chosen to be the average of the C-Pt-C angle of **1** and the H-Pt-H angle of **6**. [b] Reference 2a. [c] Reference 2c.

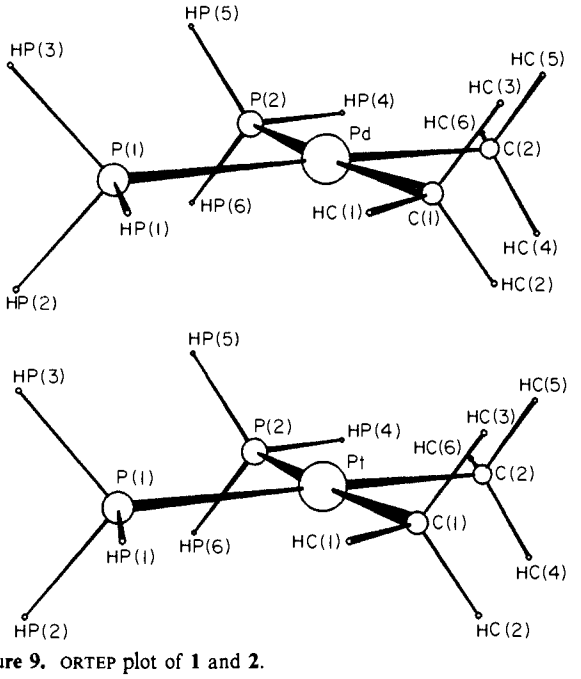

Figure 9. ORTEP plot of **1** and **2**.

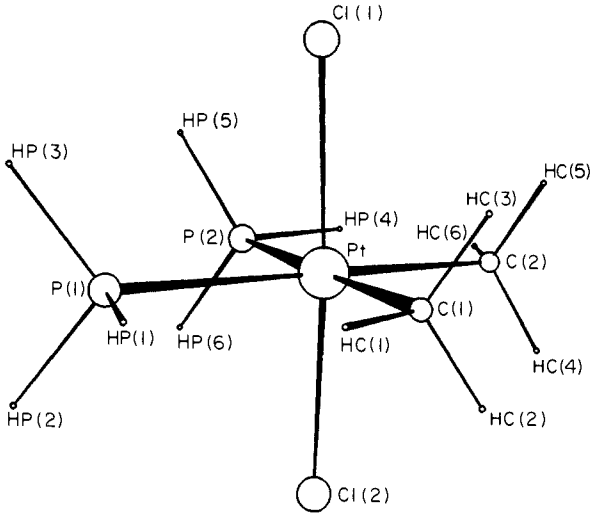

Figure 10. ORTEP plot of **3**.

coupling facile for Pd(II)[6] and unobserved for Pt(II).[10] In addition, it is known that Pt(IV) dimethyl, trimethyl, and tetramethyl complexes will reductively eliminate ethane,[7] while Pt(II) dimethyl complexes do not.[10] Our results are consistent with these experimental observations.

As indicated, the theoretical results are consistent with current experimental knowledge concerning reductive coupling and oxidative addition of Pt(II), Pd(II), and Pt(IV) complexes. These experiments can be understood on the basis of the changes in the electronic configuration of the metal plus simple ideas on the relative barriers for C-C vs. C-H vs. H-H coupling. Given the results for one metal, these ideas may be used to predict the results on other metals by using only atomic data.

D. Geometries. The geometries for all molecules studied in this work have been optimized for the HF wave functions by using analytic gradient techniques. The fully optimized HF geometries of **1** ($Pt(Me)_2(PH_3)_2$), **2** ($Pd(Me)_2(PH_3)_2$), and **3** ($Pt(Me)_2(Cl)_2(PH_3)_2$) are shown in Figures 9 and 10, and the calculational details are described in section IV. The internal coordinates around the metal atom for the complexes studied in this work are presented in Table V. Cartesian coordinates for each molecule are given in the supplementary material. We find very good agreement between our calculated geometries and X-ray structures on related molecules, as described below.

The calculated Pt-C bond distance (2.06 Å) in **1** is very close to the sum of covalent radii[16] (Pt-C sp^3) 2.09 Å and is in the range observed in X-ray structures of Pt(II) dialkyl complexes:[25] an average of 2.05 Å in Pt_2Me_4 (μ-dppm)$_2$[25c] (dppm = $Ph_2PCH_2PPh_2$); 2.18 and 2.15 Å in $PtMe_2$ (tripod) (tripod = 1,1,1-tris(diphenylphosphinomethyl)ethane);[25a] and 2.05 and 2.12 Å in $Pt(C_4H_8(PPh_3)_2$[25b].

The calculated C-Pt-C bond angle in **1** of 89° is ~10° larger than the C-Pt-C angles observed in the X-ray structures of Pt_2Me_4(μ-dppm) (81.6°) and $Pt(C_4H_8)(PPh_3)_2$ (80.9°).[25] This difference is most likely due to the PH_3 ligands having less steric bulk than substituted phosphines.

The calculated Pt-Cl bond distance in **4** of 2.35 Å and the Cl-Pt-Cl bond angle of 91° match very well with the observed Pt-Cl distances (2.368 and 2.377 Å) observed in the X-ray structure of *cis*-$Pt(PMe_3)_2Cl_2$.[26]

The calculated Pt-P bond distances are 0.1-0.2 Å longer than experiment (Pt-P = 2.23 and 2.24 Å in $PtCl_2(PMe_3)_2$[26] vs. 2.44 Å calculated for (4); 2.279 and 2.285 Å in $Pt(C_4H_8)(PPh_3)_2$[25b] vs. 2.46 Å calculated in (1)). This is systematic for Pt-P bonds at this level of calculation[2a] and may be partially due to the effect of substituted phosphines vs. PH_3. The P-Pt-P bond angle is apparently less sensitive, and good matches to the experimentally observed P-Pt-P angles are found (101° in (1) vs. 98.9° in $Pt(C_4H_8)(PPh_3)_2$ and 102° in **9** vs. 96.2° in $PtCl_2(PMc_3)_2$].[26]

Noell and Hay[4b] were the first to show that HF wave functions yield geometries of Pt and Pd complexes which compare well with X-ray structures, indicating that HF is a reasonable level of wave function with which to optimize geometries.

(25) (a) Kirchner, R. M.; Little, R. G.; Tau, K. D.; Meek, D. W. *J. Organomet. Chem.* **1978**, *149*, C15-C18. (b) Biefeld, C. G.; Eick, H. A.; Grubbs, R. H. *Inorg. Chem.* **1973**, *12*, 2166-2170. (c) Puddephatt, R. J.; Thomson, M. A.; Manojlović-Muir, L.; Muir, K. W.; Frew, A. A.; Brown, M. P. *J. Chem. Soc., Chem. Commun.* **1981**, 805-806.

(26) Del Pra, A.; Zanotti, G. *Cryst. Struct. Commun.* **1979**, *8*, 737-742.

III. Discussion

A. Effect of Added Phosphine on the Rate of Reductive Elimination. One of the unresolved questions in the experimental literature is the effect of added phosphines on the rate of C–C coupling. There are three classes of systems:

(A) For $PdMe_2L_2$[6] and $AuMe_3L$,[3b,27] experiment shows that reductive elimination of ethane is *retarded* by added phosphine. This led Hoffman et al.[3a,b] to propose a mechanism by which reductive elimination proceeds through a three-coordinate intermediate, an interpretation supported by Extended Hückel (EH) calculations.

(B) Contrasted with these results are

$$Pd(CH_3)(CH{=}CHPh)(PPh_3)_2 \rightarrow CH_3CH{=}CHPh + Pd(PPh_3)_2 \quad (32)$$

$$Ni(CH_3)_2(DIPHOS) \rightarrow Ni(DIPHOS) + C_2H_6 \quad (33)$$

(DIPHOS = $Ph_2P(CH_2)_2PPh_2$) where the addition of phosphine has no affect on the rate of C–C coupling.[28,29] These systems apparently can reductively eliminate directly from the original four-coordinate complex.

(C) There are also Ni(II) and Pt(II) complexes such as *cis*-$NiPh(CH_3)(DPE)$ (**14**) and *cis*-$Pt(C_6H_4Me\text{-}4)_2(PPh_3)_2$ (**15**), where reductive coupling of C–C bonds is *promoted* by the addition of phosphines.[11,28] This led Braterman and Cross[30] to propose a mechanism by which reductive elimination proceeds through a five-coordinate intermediate, a mechanism that was also supported by EH calculations of Tatsumi et al.[3d]

Our calculations on reductive elimination of ethane from PdR_2 and PtR_2 show that reductive elimination is favored energetically from PdR_2 because Pd prefers the d^{10} configuration.[2c] It is interesting to note that the difference in $\Delta H^{\ddagger}$ for elimination of C_2H_6 from $Pd(CH_3)_2$ and $Pt(CH_3)_2$ (30.9 kcal/mol) is very close to the difference in the driving force for each reaction (34.3 kcal/mol). This suggests that the barrier to reductive coupling of C–C bonds is strongly coupled to the driving force. Since phosphines stabilize d^{10} relative to s^1d^9, we would expect the three-coordinate complexes to have a *larger* barrier for reductive elimination than the four-coordinate complex, which should in turn have a larger barrier than the five-coordinate complex.

The consideration of only the three-coordinate intermediate for systems of class A may be an oversimplification of the real system. *Inter*molecular paths clearly are important for the decomposition of $AuMe_3L$ in some solvents (e.g., benzene, decalin, PhCl, *n*-Bu_2O, and tetrahydrofuran (THF)).[3b] More strongly coordinating solvents (Me_2SO and dimethylformamide (DMF)) appear to block intermolecular paths, resulting in very little crossover.[3b] For reductive elimination of ethane from $Pd(CH_3)_2L_2$, crossover experiments show that reductive elimination of ethane is intramolecular *only* in Me_2SO or noncoordinating solvents containing dimethyl maleate (DMM).[6] It has been assumed that DMM serves to trap the PdL_2 product before it can decompose (and thereby affect the decomposition pathway); however, Ozawa et al.[6d] have shown that variation in the concentration of DMM does not affect the rate of decomposition. (They did not report the rate with no added DMM.) This only proves that DMM is not involved in the rate-determining step of reductive elimination (which appears to be loss of a phosphine). The loss of phosphine could also be the rate-determining step in the formation of a four-coordinate intermediate in which one of the phosphines is replaced by Me_2SO, DMF, or DMM. If reductive elimination is facile from these intermediates then loss of phosphine would be the slow step which would be inhibited by added ligand.

Palladium might be expected to prefer pathways involving loss of phosphine, while other metals of the nickel triad reductively eliminate through four- and five-coordinate pathways since Pd forms weaker bonds to phosphines than Ni and Pt.[31] Apparently reductive elimination of $CH_3CH{=}CHPh$ from $Pd(CH{=}CHPh)(CH_3)(PPh_3)_2$ is *not* affected by added phosphine because the $\Delta G^{\ddagger}$ for elimination from the four-coordinate starting complex is lower than the ΔG_f of the three-coordinate intermediate.

Unfortunately it has not been possible to observe directly the three- or five-coordinate intermediates proposed for class A and C systems. Although EH calculations do support lower barriers for three- and five-coordinate complexes than four-coordinate complexes, these predicted trends in activation energies do not correlate with our observed correlation of $\Delta E^{\ddagger}$ and ΔE. EH calculations are well-known[32] not to give accurate geometries and energetics and should not be considered as proof for the proposed mechanisms. What is needed are ab initio calculations of the relative barriers of reductive elimination from three-, four-, and five-coordinate intermediates.

B. Reactivity of Metal–Carbon Bonds Involving sp^2 Hybrids vs. sp^3 Hybrids. Another trend which has been observed but not explained is the lower stability of *cis*-methylphenyl and *cis*-biphenyl complexes relative to dimethyl complexes. Reductive elimination from *cis*-$Ni(CH_3)(C_6H_5)L_2$ is faster than from *cis*-$Ni(CH_3)_2L_2$ complexes.[28] The reaction of PhLi with $PdCl_2$(DIPHOS) yields biphenyl directly, whereas MeLi reacts with $PdCl_2$(DIPHOS) to give $PdMe_2$(DIPHOS) which eliminates ethane slowly.[6a] Platinum diphenylbis(phosphine) complexes can eliminate biphenyl,[11] while platinum dimethylbis(phosphine) complexes are very stable.[10] This trend can be explained by noting that the phenyl group uses a C sp^2 hybrid orbital to form bonds, while the methyl group uses a C sp^3 hybrid orbital. The increased s character of the sp^2 hybrids causes this orbital to be less directional than the sp^3 hybrids. Therefore, the sp^2 hybrid can have more multicentered bonding at the transition state, leading to lower activation energies for CH_3—CH=CHPh, CH_3—Ph, and Ph—Ph coupling.

It should be noted the Ph–CH_3 and Ph–Ph bond energies are 11.4[19b] and 26 kcal/mol stronger[9c] than the H_3C–CH_3 bond energy (90.4 kcal/mol).[19b] Thus, *if* the Mt–CH_3 and Mt–Ph bond energies were approximately the same, this would lead to a larger driving force for reductive elimination of sp^2 species. Evans et al. have made a thermochemical estimate for the Pt–Ph bond energy of 63.1[33] that is 7 kcal/mol stronger than our calculated Pt–CH_3 intrinsic bond energy. This value for the bond energy is, however, strongly dependent on their estimated Pt–Cl bond energy in $PtCl_2(PPh_3)_2$ (which was assumed to be the same as the Pt–Cl bond energy in $PtCl_2$), which could easily cause errors of ~10 kcal/mol. Therefore, there currently are insufficient data to determine whether the diphenyl and methylphenyl Pt complexes are less stable thermodynamically than the dimethyl complex.

Thermochemical data[34] from $ThR_2(Cp^*)_2$ complexes demonstrate that Th–Ph bond energies are 13 kcal/mol stronger than Th–CH_3 bond energies. Therefore, it does appear that diphenyl and methylphenyl complexes have approximately the same enthalpy for reductive elimination as dimethyl complexes.

Either of the above interpretations for the increased lability of sp^2 vs. sp^3 carbons would suggest that alkynyl groups will reductively eliminate faster than phenyl or vinyl groups. Indeed, Ph—C≡C—C≡C—Ph has been indentified in the decomposition products of *cis*-$Pt(C{\equiv}C{-}Ph)_2L_2$.[35] A more careful analysis of the decomposition of dialkynyl complexes should help establish the trend of sp hybridization vs. rate of reductive elimination.

C. Heat of Formation of Pt(II) and Pd(II) Salts. We have found that the difference in enthaplies ($\Delta(\Delta H)$) for reductive elimination from the corresponding Pt(II) and Pd(II) compounds

(27) Tamaki, A.; Magennis, S. A.; Kochi, J. K. *J. Am. Chem. Soc.* **1974**, *96*, 6140–6148.
(28) Komiya, S.; Abe, Y.; Yamamoto, A.; Yamamoto, T. *Organometallics* **1983**, *2*, 1466–1468.
(29) Kohara, T.; Yamamoto, T.; Yamamoto, A. *J. Organomet. Chem.* **1980**, *192*, 265–274.
(30) Braterman, P. S.; Cross, R. J. *Chem. Soc. Rev.* **1973**, *2*, 271–294.
(31) Basolo, F. *Trans. N. Y. Acad. Sci.* **1969**, *3*, 676–685.
(32) Levine, I. N. *Quantum Chemistry*, 2nd ed.; Allyn and Bacon: Boston, MA, 1974; pp 450–452.
(33) (a) Evans, A.; Mortimer, C. T.; Puddephat, R. J. *J. Organomet. Chem.* **1975**, *96*, C58–C60. (b) Ashcroft, S. J.; Mortimer, C. T. *J. Chem. Soc. A* **1967**, 930–931.
(34) Bruno, J. W.; Marks, T. J.; Morss, L. R. *J. Am. Chem. Soc.* **1983**, *105*, 6824–6832.
(35) Collamati, I.; Furlani, A. *J. Organomet. Chem.* **1969**, *17*, 457–461.

Table VI. Enthalpies (kcal/mol at 298 K) for Pt(II) and Pd(II) Salts[a]

compd.	$\Delta H_f^0[PtX_2(s)]$	$\Delta H_f^0[PdX_{2(s)}]$	$\Delta H[Pt_{(g)}(^1S) + X_{2(g)} \rightarrow PtX_2(s)]$[c]	$\Delta H[Pd_{(g)}(^1S) + X_{2(g)} \rightarrow PdX_{2(s)}$	$\Delta(\Delta H)$
$Mt(OH)_2$[b]	-84	-88	-184[b]	-148	36
$MtCl_2$	-33	-39	-166	-132	34
$MtBr_2$	-15	-25	-148	-118	30

[a] All ΔH_f are from ref 36, except as noted. [b] $\Delta H_{f298}(H_2O_2) = -32.53$ kcal/mol: Stull, D. R.; Prophet, H. *JANAF Thermochemical Tables*, 2nd ed.; National Bureau of Standards: Washington, DC, June 1971; NSRDS-NBS 37. [c] $\Delta H_{sub}(Pt) = 121.6$ kcal/mol at 25 °C,[36] $\Delta E(^3D \rightarrow {}^1S) = 11.0$ kcal/mol;[18] consequently, $\Delta H_f^0[Pt_{(g)}(^1S)] = 121.6 + 11.0 = 132.6$ kcal/mol. [d] $\Delta H_{sub}(Pd) = 92.96$ kcal/mol.[36] The ground state of Pd is ^1S; therefore, $\Delta H_{sub}(Pd) = \Delta H_f^0[Pd_{(g)}(^1S)]$.

is always within 5 kcal/mol of the difference in the $s^1d^9 \rightarrow d^{10}$ splittings for these metals (33 kcal/mol).[18] Unfortunately, there are no reliable $\Delta H_f°$'s for Pt and Pd complexes available in the literature to provide a test of this theoretical trend. However, $\Delta H_f°$'s for various Pt(II) and Pd(II) salts are available.[36] Since Pt and Pd have the same covalent radii and electronegativities,[16] we can assume that the lattice energies for the corresponding PtX_2 and PdX_2 salts are the same. Therefore, the $\Delta(\Delta H)$ for the reaction $Mt(^1S)_{(g)} + X_{2(g)} \rightarrow MtX_{2(s)}$ should also be approximately equal to 33 kcal/mol. Indeed, as indicated in Table VI, the experimental $\Delta(\Delta H)$'s are 33 ± 3 kcal/mol, in excellent agreement with our prediction.

The alternative interpretation based on an ionic model for Mt–C bonds would suggest that the $\Delta(\Delta H)$ is equal to the difference in the sums of the first and second ionization potentials for Pt and Pd.[18] This would predict a $\Delta(\Delta H)$ of 15 kcal/mol instead of 33 kcal/mol. Therefore, our covalent bonding model is far more consistent with the experimentally observed $\Delta H_f°$ for these salts.

D. **Comparison with Other Theoretical Studies.** Hoffmann et al.[3a] analyzed Extended Hückel (EH) calculations on reductive elimination from complexes of the Ni triad to obtain five conclusions concerning these reactions, the first three of which are relevant to this work since they concern reductive elimination from dimethylbis(phosphine) complexes.[37] Hoffman et al. stated these rules to be the following:

1. The better the σ-donating capability of the leaving groups, the more readily the elimination reaction proceeds.
2. Stronger donor ligands that are trans to the leaving groups give a higher barrier for the elimination reaction.
3. Increased stability of the MA_2 orbital [where A indicates modified hydrogens used to model phosphines] facilitates the reductive elimination of D_2 [where D is a modified hydrogen used to model CH_3 groups]. A lower energy for the b_2 orbital of MA_2 results from a more stable metal d orbital.[3a]

Since we find essentially covalent bonding in Pt and Pd complexes, a better σ-donor leaving group is equivalent to a leaving group with lower electronegativity. Leaving groups (R) with higher electronegativities would help stabilize the s orbital of the metal atom by increasing the amount of s character in the metal sd hybrid orbital used in the M–R bond. This will stabilize the s^1d^9 configuration of the metal atom and reduce the driving force for reductive elimination. This is in agreement with Hoffmann's first conclusion.

We have not made systematic variations in the ligands; however, the trends in going from no ligands (a very weak donor!) to two PH_3 groups are quite suggestive. We find that (due to the overlap between the phosphine lone pairs and the metal s orbital) the sd hybrid orbital used in the M–R bond has to build in p character to stay orthogonal to phosphine lone pairs. This increased p character makes the intrinsic M–R bond strengths slightly stronger, as expected from simple valence bond calculations.[15] The σ-donating ability of substituted phosphine ligands is directly related to the overlap between the ligand lone pair and metal s orbital. The stronger the donor, the larger the overlap. The larger overlap will lead to stronger M–R bonds which may cause the barriers for reductive elimination to be higher. Therefore, our results are also consistent with the second conclusion of Hoffmann.

However, we believe that Hoffmann's third conclusion, although reasonable, does not present the complete picture. We find that the important issue here is the relative energy of the s^1d^9 and d^{10} configurations (VB language) or in MO language the relative energy of the valence s and d orbitals of the metal atom and not just the d orbital energy. The d^{10} configuration is stabilized relative to s^1d^9 by destabilizing the s orbital relative to the d orbital. Stabilization of the d^{10} configuration leads to larger driving forces and lower barriers for reductive elimination. We have shown in an earlier paper that reductive coupling of C–C bonds from $PdMe_2$ is favored over $PtMe_2$, both kinetically and energetically. This dramatic difference arises because relative to Pt, Pd has a 33 kcal/mol bias for the d^{10} state. This effect is much more dramatic than the other two and should dominate the stability of the these complexes.

Related trends were also observed in the CNDO calculations of Gritsenko et al.[4j] where the stability of the $MH_2(PH_3)_2$ complexes (Mt = Pd or Pt) was correlated with the Mt s character of the wave function.

Other ab initio theoretical calculations involving square-planar complexes of the Ni triad include studies of $NiMe_2(H_2O)_2$ by Åkermark et al.[4e] and $PdH_2(H_2O)_2$ by Siegbahn et al.[5e] In both of these studies, H_2O was used as a model ligand. Åkermark et al.[4e] found little change in the d orbital occupations upon addition of H_2O ligands, and Siegbahn actually found a small stabilization (~5 kcal/mol)[38] of the s^1d^9 singlet vs. the d^{10} singlet of $Pd(H_2O)_2$ relative to the atomic state splittings of Pd. The differences between these previous studies and ours probably results from their use of H_2O ligands rather than PH_3. The lone pairs of H_2O are much smaller than the lone pair of PH_3. The overlap between the lone pairs of H_2O and the Pd 5s orbital is probably much smaller than for phosphine lone pairs. This would lead to a smaller destabilization of the s orbital, favoring the s^1d^9 configuration over d^{10} (Pd and Pt prefer "softer" ligands such as PR_3 over H_2O). The relevant experiments all involve complexes with phosphine ligands, and hence our studies using phosphines are more pertinent for understanding the observed trends in C–C coupling.

IV. Calculational Details

A. Basis Sets and Effective Potentials. The basis sets and relativistic effective potentials used in this study for Pd and Pt are those of Hay et al.[4b] The basis on carbon is the Dunning double-ζ contraction of the Huzinaga (9s5p) basis.[39] The effective potential for phosphorus is the SHC potential of Rappé et al.[40] The SHC basis for the phosphorus atom[40] was contracted to a minimum basis set by using atomic calculations. Three different basis sets were used on the hydrogen atoms depending on their chemical environment. For hydrogen atoms bound to phosphorus, we used a minimum basis set contraction of the Huzinaga four-Gaussian hydrogen basis (no scaling).[41] Methyl protons were de-

(36) Hartley, F. R. *The Chemistry of Platinum and Palladium*; Wiley: New York, 1973; Chapter 2.

(37) The last two conclusions concern the three-coordinate intermediates resulting from loss of phosphine from the square-planar complexes.

(38) This stabilization energy was derived from the results of Siegbahn et al.[5e] by summing the energy needed to bend the O–Pd–O angle in $Pd(OH_2)_2$ from its equilibrium value of 180° to 90° (15 kcal/mol) and the diabatic $d^{10} \rightarrow s^1d^9$ singlet splitting for $Pd(OH_2)_2$ (20 kcal/mol), at a 90° O–Pd–O angle to give an adiabatic splitting of 35 kcal/mol. This splitting is 5 kcal/mol smaller than their calculated $d^{10} \rightarrow s^1d^9$ splitting for Pd atom of 40 kcal/mol.

(39) Dunning, T. H., Jr.; Hay, P. J. In *Modern Theoretical Chemistry: Methods of Electronic Structure Theory*; Schaefer, H. F., III, Ed.; Plenum: New York, 1977; Vol. 3, Chapter 4, pp 79–127.

(40) Rappé, A. K.; Smedley, T. A.; Goddard, W. A., III *J. Phys. Chem.* **1981**, *85*, 1662–1666.

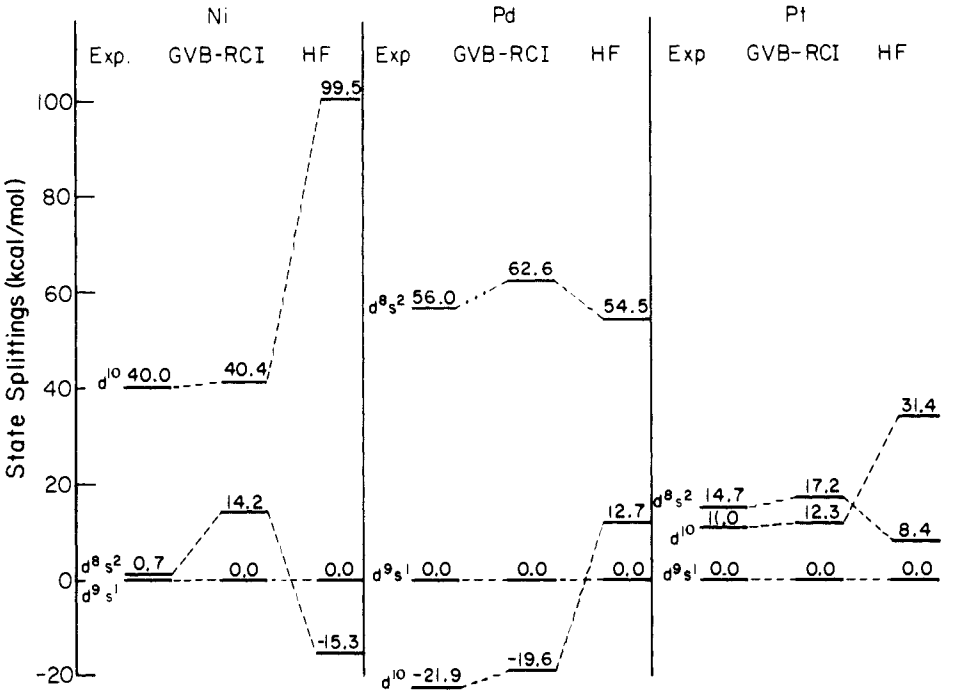

Figure 11. Atomic excitation energies for Ni, Pd, and Pt. All quantities in kilocalories/mole.

scribed by using a double-ζ contraction of the Huzinaga four-Gaussian basis scaled by a factor of 1.2.[39] The active hydrogen bound to the metal atoms in the $Pt(H)(Me)(PH_3)_2$ and $Pt(H)_2(PH_3)_2$ complexes was treated with a triple-ζ contraction of the Huzinaga six-Gaussian basis.[41] This was necessary to allow the hydrogen to adjust for optimum bonding to the metal atom in the reactant and optimum bonding to the methyl group or H atom in the products. The chlorine potential was the SHC potential of Rappé et al.,[40] and the double-ζ contraction of the SHC basis[40] was used.

The effective potentials for P, Cl, Pt, and Pd are expected to provide ab initio quality descriptions for these atoms. Good measures for the quality of description for Pd and Pt are the atomic-state splittings as indicated in Figure 11. For highly accurate calculations, polarization functions (p's on H, d's on C, P, and Cl, f's on Pt or Pd) are needed. This will lead to stronger intrinsic bond energies but will probably have little effect on the ΔE for oxidative addition/reductive elimination reactions (since bonds of reactant and product are affected similarly). The major factor in understanding these reactions is that the s^1d^9–d^{10} splitting of the metal atoms be accurately described.[2] Although the level of basis can certainly be improved, it should be quite adequate for the purposes here, namely, the conceptual description of the differences between Pt(II), Pt(IV), and Pd(II) complexes.

B. Geometries. All geometries of the various complexes were fully optimized at the HF level using analytic energy gradients and the Newton–Raphson procedure.[42] For the calculations on the triplet states of ML_2 and MCl_2L_2, the geometries were frozen at the geometry of the fragment in the corresponding MR_2L_2 or $MR_2Cl_2L_2$ complex. This was done so that geometric relaxation energies would not be included in calculating intrinsic bond energies.

C. Wave Functions. All energetics reported here involve the GVB description of electron correlation for the important valence electrons. For an electron pair that would be described as doubly occupied in HF theory, the GVB description would allow two orbitals each optimized self-consistently with all other orbitals of the molecules

$$\phi^{HF}(1,2) = \varphi(1)\varphi(2)(\alpha\beta - \beta\alpha) \rightarrow \phi^{GVB}(1,2) = [\varphi_a(1)\varphi_b(2) + \varphi_b(1)\varphi_a(2)](\alpha\beta - \beta\alpha) \quad (34)$$

When there are additional electron pairs, each may be correlated as in (34) so that the doubly occupied orbitals φ_1, φ_2, etc., of an HF wave function become singly occupied orbitals (as in (34)), φ_{1a}, φ_{1b}, φ_{2a}, φ_{2b} of the GVB wave function. Although for HF wave functions the doubly occupied orbitals can generally be taken as either delocalized (canonical) or localized, the GVB orbitals are uniquely determined and are generally localized (reminiscent of simple valence bond theory). The general form of a GVB wave function is

$$\alpha[(\varphi_{1a}\varphi_{1b}\varphi_{2a}\varphi_{2b}\cdots)\chi] \quad (35)$$

where χ is an appropriate optimized spin function for N electrons. However, when the GVB orbitals are calculated, it is generally convenient to choose χ as the simple valence bond function (perfect pairing)

$$\chi^{VB} = (\alpha\beta - \beta\alpha)(\alpha\beta - \beta\alpha)\cdots \quad (36)$$

In this case the orbitals for different electron pairs are taken as orthogonal, and the resulting orbitals are denoted as GVB-PP to indicate the restricted form of the wave function. If 5 pairs of electrons are so correlated (using 10 orbitals), the wave function is denoted as GVB-PP(5/10); however, other orbitals of the wave function are understood to be calculated self-consistently. (This wave function would involve $2^5 = 32$ different orbital configurations.) Such wave functions quite accurately describe systems where one valence bond structure is adequate (no resonance); however, for transition-metal systems, spin couplings other than (36) are often important. These spin-coupling effects are usually accurately described using the GVB-PP orbitals but allowing the two electrons of each orbital pair to be either in different orbitals (as in (34)) or in the same orbital (e.g., $\varphi_a(1)\varphi_a(2)$). Allowing a similar description for all correlated pairs leads to the GVB-RCI wave function. Since there are three orbital products for each pair of electrons, the GVB-RCI(5/10) wave function has $3^5 = 243$ orbital products. In addition to an optimized spin coupling, the RCI wave function includes important electron correlation effects in which two electrons in one bond pair can respond instantaneously to the motions of two electrons in another bond pair (interpair correlation). The orbitals of the GVB-RCI wave function can be solved self-consistently; however, it is generally adequate to use the orbitals of the GVB-PP wave function, and we have found this to be the case for complexes of the type studied in this paper. For cases where *resonance* of simple valence bond structures would be important, it is often essential to allow readjustments in those bond pairs that would change in the resonance. Thus, for reductive C–C coupling, the two localized M–C pairs change into a C–C bond pair and a metal d pair as

(41) Huzinaga, S. *J. Chem. Phys.* **1965**, *42*, 1293–1302.

(42) All of the geometry optimizations were obtained by using an analytic gradient program (GVBGRAD). This program was based on subroutines from (a) the GVB2P5 program (Bobrowicz, F. W.; Goddard, W. A., III In *Modern Theoretical Chemistry: Methods of Electronic Structure Theory*; Schaefer, H. F., III, Ed.; Plenum: New York, 1977; Vol. 3, Chapter 4, pp 79–127) to evaluate density matrices for restricted HF and GVB-PP wave functions, (b) the HONDO program (Dupuis, M.; King, H. F. *J. Chem. Phys.* **1978**, *68*, 3998–4004) to calculate derivatives of the ab initio terms in the energy expression, and (c) routines from the GAUSSIAN 80 program (Binkely, J. W.; Whitesides, R. A.; Krishnan, R.; Seeger, R.; DeFrees, D. J.; Schlegel, H. B.; Topiol, S.; Kahn, L. R.; Pople, J. A. GAUSSIAN 80; Department of Chemistry, Carnegie-Mellon University: Pittsburgh, PA, 1980) to calculate the effective potential terms of the derivative. To determine the step size taken each iteration, we used a relatively simple Newton–Raphson technique in which the second derivative matrix is updated after every gradient calculation (except for the starting geometry) (Low, J. J.; Goddard, W. A., III, unpublished results).

the bond is broken, and resonance between these configurations is important. In this case we refine the GVB-RCI(2/4) description of these two pairs by using the GVB-CI(2/4) description, where all four electrons are allowed to occupy all four orbitals in any way (leading to 19 orbital products).

We find (see Figure 11) for Ni, Pd, and Pt that the GVB description (which uses 10 optimized orbitals for all states) leads to a rather accurate description of the relative energies for the d^{10}, s^1d^9, and s^2d^8 configurations and is particularly accurate for s^1d^9 vs. d^{10}, the states relevant for this paper. For the s^2d^8 states the s^2 pair was polarized in the $\pm z$ directions, and d_{z^2} and the d_{xy} were singly occupied.

For the various $M(R_1)(R_2)$ complexes, it is necessary to correlate not only the 10 metal valence electrons but also the additional electrons involved in the covalent $M-R_1$ and $M-R_2$ bonds. Thus, a total of 12 electrons or 6 electron pairs must be correlated. Consequently, we first carried out GVB-PP(6/12) calculations using 12 orbitals to correlate the motions of these 6 pairs (12 electrons). (All other orbitals are doubly occupied but are solved self-consistently.) In order to include the spin-coupling, interpair correlation, and resonance effects,[2a,c] the energetics reported here were determined at the GVB-CI(2/4) × RCI(4/8) level.

In *previous studies* of the reaction path for reductive coupling, the necessity for the simultaneous description of both the reactant (s^1d^9) and the product (d^{10}) resonance structures in the transition-state region required the use of three orbitals (rather than two) for each of the two bond pairs that change during the reaction.[2] Thus, rather than GVB-PP(2/4), these two electron pairs were described with GVB-PP(2/6). In order to allow a full description of resonance effects in the transition state, all occupations of these six orbitals were allowed for all four electrons, denoted as GVB-CI(2/6). The other four pairs of electrons were correlated as usual, leading to a composite wave function of the form GVB-CI(2/6) × RCI(4/8). We also optimized the orbitals at this level. In the *current study*, the main interest is in overall energy differences between products and reactants, where this resonance is not so important. Consequently, we use only two orbitals for these bond pairs, and the orbitals were optimized at the GVB-PP level. However, as in the previous studies, we carry out a full CI among the (four) orbitals involving those two bond pairs (CI(2/4)). Thus the wave function used in these studies is GVB-CI(2/4) × RCI(4/8).

Acknowledgment. This work was supported in part by a grant from the National Science Foundation (No. CHE83-18041). J.J.L. acknowledges financial support in the form of fellowships from Exxon and ARCO.

Registry No. **1**, 79232-18-1; **2**, 79218-06-7; **3**, 103191-78-2; **4**, 79329-16-1; **5**, 79232-17-0; **6**, 76832-29-6; **7**, 76830-85-8; **8**, 78452-79-6.

Supplementary Material Available: Cartesian coordinates for Pt- and $Pd(CH_3)_2(PH_3)_2$, $PtCl_2(CH_3)_2(PH_3)_2$, $PtCl_2(PH_3)_2$, $Pt(H)(CH_3)(PH_3)_2$, and Pt- and $Pd(PH_3)_2$ and internal coordinates of methyls and phosphines (8 pages). Ordering information given on any current masthead page.

Ribose Puckering: Structure, Dynamics, Energetics, and the Pseudorotation Cycle

Stephen C. Harvey* and M. Prabhakaran

Contribution from the Department of Biochemistry, The University of Alabama at Birmingham, Birmingham, Alabama 35294. *Received October 2, 1985*

Abstract: We have examined the pucker dependence of ribose structure and ribose conformational energy in a set of 4800 configurations generated during a 304-K, 24-ps, in vacuo molecular dynamics simulation of phenylalanine transfer RNA. This data set spans all of the thermodynamically accessible regions of the northern (N), eastern (E), and southern (S) quadrants of the traditional polar representation of sugar pucker conformational space. Spontaneous repuckering, with passage between the minimum energy configurations at C2′-endo (S) and C3′-endo (N), occurs for riboses in single-stranded and loop regions with an observed frequency of about 1 ns^{-1}, and the lowest energy barrier is observed at O4′-endo, so repuckering is via the N–E–S pathway, as expected. The pseudorotational description of sugar pucker is found to be reasonably accurate, although we find a small dependence of pucker amplitude (θ_m) on pucker phase angle (P), and there are substantial fluctuations in θ_m at any given value of P. The three pseudorotation formalisms (Altona–Sundaralingam, Rao–Westhof–Sundaralingam, and Cremer–Pople) give only small differences when characterizing a given configuration, and we discuss relationships for interconverting between the formalisms. On examining our potential energy function, we find that the most important contributions to the shape of the conformational energy curve arise from the torsional energy terms. For examining questions of structure and for comparing different potential energy functions, molecular dynamics is a useful complement to energy minimization, because of the very large number of configurations that are generated, and because these configurations represent all thermally accessible states.

The central role of the furanose ring in the conformation of nucleic acids has long been recognized. The global conformation of the molecule is affected by sugar conformation in two ways. First, the backbone which connects successive phosphate atoms passes through the furanose ring. Second, the base is covalently bonded to the C1′ atom in the ring. Thus, the geometry of the sugar (ribose in RNAs, deoxyribose in DNAs) is one of the critical factors for determining the overall molecular architecture. It is also likely that changes in the conformation of sugars will play a fundamental role in the dynamic aspects of nucleic acid structures, a subject of increasing interest.

One of the most important features of furanose conformation is the sugar pucker, which arises because the five-membered ring would be highly strained if it were held in a planar configuration. A number of methods to mathematically describe the deviation of closed cyclic rings from planarity have been given.[1-5] Although their details differ (see Methods), they all describe the ring conformation in terms of a puckering phase angle, P, identifying which part of the ring is farthest from planarity, and an amplitude, measuring the magnitude of the deviation from planarity. Amplitude is denoted θ_m if pucker is defined in terms of ring torsion

(1) Kilpatrick, J. E.; Pitzer, K. S.; Spitzer, R. *J. Am. Chem. Soc.* **1947**, *69*, 2483-2488.
(2) Geise, H. J.; Altona, C.; Romers, C. *Tetrahedron Lett.* **1967**, *15*, 1383-1386.
(3) Altona, C.; Sundaralingam, M. *J. Am. Chem. Soc.* **1972**, *94*, 8205-8212.
(4) Cremer, D.; Pople, J. A. *J. Am. Chem. Soc.* **1975**, *97*, 1354-1358.
(5) Rao, S. T.; Westhof, E.; Sundaralingam, M. *Acta Crystallogr., Sect. A: Found. Crystallogr.* **1981**, *37*, 421-425.

0002-7863/86/1508-6128$01.50/0